IOPscience iopscience.iop.org

Home Search Collections Journals About Contact us My IOPscience

The Monge metric on the sphere and geometry of quantum states

This article has been downloaded from IOPscience. Please scroll down to see the full text article.

2001 J. Phys. A: Math. Gen. 34 6689

(http://iopscience.iop.org/0305-4470/34/34/311)

View the table of contents for this issue, or go to the journal homepage for more

Download details:
IP Address: 171.66.16.97
The article was downloaded on 02/06/2010 at 09:11

Please note that terms and conditions apply.

INSTITUTE OF PHYSICS PUBLISHING JOURNAL OF PHYSICS A: MATHEMATICAL AND GENERAL

J. Phys. A: Math. Gen. **34** (2001) 6689–6722 PII: S0305-4470(01)18080-7

The Monge metric on the sphere and geometry of quantum states

Karol Życzkowski[1,2] **and Wojciech Słomczyński**[3]

[1] Centrum Fizyki Teoretycznej, Polska Akademia Nauk, Al. Lotników 32, 02-668 Warszawa, Poland
[2] Instytut Fizyki im. Mariana Smoluchowskiego, Uniwersytet Jagielloński, ul. Reymonta 4, 30-059 Kraków, Poland
[3] Instytut Matematyki, Uniwersytet Jagielloński, ul. Reymonta 4, 30-059 Kraków, Poland

E-mail: karol@cft.edu.pl and slomczyn@im.uj.edu.pl

Received 18 October 2000, in final form 14 June 2001
Published 17 August 2001
Online at stacks.iop.org/JPhysA/34/6689

Abstract

Topological and geometrical properties of the set of mixed quantum states in the N-dimensional Hilbert space are analysed. Assuming that the corresponding classical dynamics takes place on the sphere we use the vector $SU(2)$ coherent states and the generalized Husimi distributions to define the Monge distance between two arbitrary density matrices. The Monge metric has a simple semiclassical interpretation and induces a non-trivial geometry. Among all pure states the distance from the maximally mixed state ρ_*, proportional to the identity matrix, admits the largest value for the coherent states, while the delocalized 'chaotic' states are close to ρ_*. This contrasts the geometry induced by the standard (trace, Hilbert–Schmidt or Bures) metrics, for which the distance from ρ_* is the same for all pure states. We discuss possible physical consequences including unitary time evolution and the process of decoherence. We introduce also a simplified Monge metric, defined in the space of pure quantum states and more suitable for numerical computation.

PACS numbers: 03.65.Bz, 05.45+b

1. Introduction

Consider two quantum states described by the density matrices ρ_1 and ρ_2. What is their distance in the space of quantum states? One should not expect a unique, canonical answer for this question. In contrast, several possible distances can be defined, related to different metrics in this space. As usual, each solution possesses some advantages and some drawbacks; each might be useful for different purposes.

Perhaps the simplest possible answer is given by the norm of the difference. The trace norm leads to the *trace distance*

$$D_{\mathrm{tr}}(\rho_1, \rho_2) = \mathrm{tr}\sqrt{(\rho_1 - \rho_2)^2} \tag{1.1}$$

 © 2001 IOP Publishing Ltd Printed in the UK

used by Hillery [1, 2] to describe the non-classical properties of quantum states and by Englert [3] to measure the distinguishability of mixed states. In a similar way the Frobenius norm results in the *Hilbert–Schmidt distance*

$$D_{\mathrm{HS}}(\rho_1, \rho_2) = \sqrt{\mathrm{tr}[(\rho_1 - \rho_2)^2]} \tag{1.2}$$

often used in quantum optics [4–6].

Another approach based on the idea of *purification* of a mixed quantum state leads to the *Bures distance* [7, 8]. An explicit formula for the Bures distance was found by Hübner [9]

$$D_{\mathrm{Bures}}(\rho_1, \rho_2) = \sqrt{2\big(1 - \mathrm{tr}[(\rho_1^{1/2}\rho_2\rho_1^{1/2})^{1/2}]\big)} \tag{1.3}$$

and various properties of this distance are a subject of a considerable interest (see [10–16]). It was shown by Braunstein and Caves [17] that for neighbouring density matrices the Bures distance is proportional to the statistical distance introduced by Wootters [18] in the context of measurements which optimally resolve neighbouring quantum states.

Note that for pure states $\rho_1 = |\varphi_1\rangle\langle\varphi_1|$ and $\rho_2 = |\varphi_2\rangle\langle\varphi_2|$ we can easily calculate the above standard distances, namely

$$D_{\mathrm{tr}}(|\varphi_1\rangle, |\varphi_2\rangle) = 2\sqrt{1-p} \tag{1.4}$$

$$D_{\mathrm{HS}}(|\varphi_1\rangle, |\varphi_2\rangle) = \sqrt{2\,(1-p)} \tag{1.5}$$

and

$$D_{\mathrm{Bures}}(|\varphi_1\rangle, |\varphi_2\rangle) = \sqrt{2\left(1 - \sqrt{p}\right)} \tag{1.6}$$

where the 'transition probability' $p = |\langle\varphi_1|\varphi_2\rangle|^2 = \cos^2(\Xi/2)$. The angle Ξ is proportional to the Fubini–Study distance $D_{\mathrm{FS}}(\varphi_1, \varphi_2)$ in the space of pure states, and for $N = 2$ it is just the angle between the corresponding points of the Bloch sphere [19]. The Fubini–Study metric defined by

$$D_{\mathrm{FS}}(\varphi_1, \varphi_2) = \tfrac{1}{2}\arccos(2p - 1) = \arccos\sqrt{p} \tag{1.7}$$

corresponds to the geodesic distance in the complex projective space (see e.g. [19]) and for infinitesimally small values of p becomes proportional to any of the standard distances.

In a recent paper [20] we introduced the *Monge metric* D_{M} in the space of density operators belonging to an infinite-dimensional separable Hilbert space $\mathcal{H}$. The Monge metric fulfils the following *semiclassical property*: the distance between two harmonic oscillator (Glauber) coherent states $|\alpha_1\rangle$ and $|\alpha_2\rangle$ localized at points a_1 and a_2 of the classical phase space $\Omega = \mathbb{C}$ is equal to the Euclidean distance d between these points

$$D_{\mathrm{M}}(|\alpha_1\rangle, |\alpha_2\rangle) = d(a_1, a_2). \tag{1.8}$$

In the semiclassical regime this condition is rather natural, since the quasi-probability distribution of a quantum state tends to be strongly localized in the vicinity of the corresponding classical point. A motivation to study such a distance stems from the search for the quantum Lyapunov exponent, where a link between distances in the Hilbert space and in the classical phase space is required [21]. Our construction was based on the Husimi representation of a quantum state ρ given by [22]

$$H_\rho(\alpha) := \frac{1}{\pi}\langle\alpha|\rho|\alpha\rangle \tag{1.9}$$

for $\alpha \in \mathbb{C}$. The Monge distance D_{M} between two arbitrary quantum states was defined as the Monge–Kantorovich distance between the corresponding Husimi distributions [20].

Although the Monge–Kantorovich distance is not easy to calculate for two- or higher-dimensional problems, it satisfies the semiclassical property (1.8), crucial in our approach. On

the other hand, one could not use for this purpose any 'simpler' distances between the Husimi distributions, for example L_1 or L_2 metrics, because the semiclassical property does not hold in these cases. Moreover, this property is not fulfilled for any of the standard distances in the space of density matrices (trace, Hilbert–Schmidt or Bures distances). Consider two arbitrary pure quantum states $|\varphi_1\rangle$ and $|\varphi_2\rangle \in \mathcal{H}$ and the corresponding density operators $\rho_1 = |\varphi_1\rangle\langle\varphi_1|$ and $\rho_2 = |\varphi_2\rangle\langle\varphi_2|$. If the states are orthogonal, the standard distances between them do not depend on their localization in the phase space. For example the Hilbert–Schmidt and the Bures distances between two different Fock states $|n\rangle$ and $|m\rangle$ are equal to $\sqrt{2}$, and the trace distance is equal to 2. Although the state $|1\rangle$ is localized in the phase space much closer to the state $|2\rangle$ than to $|100\rangle$, this fact is not reflected by any of the standard distances. Clearly, the same concerns a nonlinear function of the Hilbert–Schmidt distance, which satisfy the semiclassical condition (1.8) and was recently introduced in [23]. On the other hand, the Monge distance is capable of revealing the phase space structure of the quantum states, since $D_{\mathrm{M}}(|m\rangle, |n\rangle) = |a_m - a_n|$, where $a_k = \sqrt{\pi}\binom{2k}{k}(2k+1)/2^{2k+1} \sim \sqrt{k}$ (see [20]).

In this paper we propose an analogous construction for a classical compact phase space and the corresponding finite-dimensional Hilbert spaces $\mathcal{H}_N$. In particular we discuss the $N = (2j+1)$-dimensional Hilbert spaces generated by the angular momentum operator J. In the classical limit the quantum number j tends to infinity and the classical dynamics takes place on the sphere S^2 the radius of which we set to unity. However, the name *Monge metric on the sphere* should not be interpreted literally: the metric is defined in the space of density matrices, while the connection with the sphere is obtained via the $SU(2)$ vector coherent states, used in the construction to represent a quantum state by its generalized Husimi distribution. In general, the Monge distance in the space of quantum states can be defined with respect to an arbitrary classical phase space Ω.

This paper is organized as follows. In section 2 we review some properties of pure and mixed quantum states in a finite-dimensional Hilbert space. In section 3 we recall the definition of the Monge metric based on the Glauber coherent states and extend this construction to an arbitrary set of (generalized) coherent states. We analyse basic properties of such a defined metric and its relation to other distances in the space of density operators. The case where the classical phase space is isomorphic with the sphere S^2, corresponding to the $SU(2)$ coherent states, is considered in section 4. We compute the Monge distance between certain pure and mixed states, and compare the results with other distances (trace, Hilbert–Schmidt, and Bures). In particular, we give the formulae for the Monge distance between two coherent states (for arbitrary j) and between two arbitrary mixed states for $j = 1/2$. In the latter case the geometry induced by the Monge distance coincides with the standard geometry of the Bloch ball induced by the Hilbert–Schmidt (or the trace) distance. However, in the higher dimensions both geometries differ considerably. Potential physical consequences of our approach are discussed in section 5. In section 6 we introduce a simplified version of the Monge metric, defined only in the space of pure quantum states, but better suited for numerical computation. Finally, some concluding remarks are provided in section 7.

2. Space of mixed quantum states

2.1. Topological properties

Let us consider a *pure quantum state* $|\psi\rangle$ belonging to an N-dimensional Hilbert space $\mathcal{H}_N$. It may be described by a normalized vector in $\mathcal{H}_N$, or by the density matrix $\rho_\psi = |\psi\rangle\langle\psi|$. Such a state fulfills the purity condition: $\rho_\phi^2 = \rho_\phi$. The manifold $\mathcal{P}$, containing all pure states, is homeomorphic with the complex projective space $\mathbb{C}P^{N-1}$. This space is $2(N-1)$

dimensional. In the simplest case $N = 2$, the two-dimensional space $\mathbb{C}P^1$ corresponds to the *Bloch sphere*.

To generalize the notion of pure states one introduces the concept of *mixed quantum states*. They are represented by $N \times N$ positive Hermitian matrices ρ, which satisfy the trace condition $\operatorname{tr}\rho = 1$. Any density matrix may be diagonalized and represented by

$$\rho = VEV^\dagger \tag{2.1}$$

where V is unitary, while a diagonal matrix of eigenvalues E contains only non-negative entries: $E_i \geqslant 0$; $i = 1, \ldots, N$. For each pure state all entries of E are equal to zero, but one equal to unity. Due to the trace condition $\sum_{i=1}^{N} E_i = 1$. This means that the set of all such matrices E forms an $(N-1)$-dimensional simplex $\mathcal{S}_N$ in $\mathbb{R}^N$. Let B be a diagonal unitary matrix. Since

$$\rho = VEV^\dagger = VBEB^\dagger V^\dagger \tag{2.2}$$

the matrix V is determined up to N arbitrary phases entering B. On the other hand, the matrix E is defined up to a permutation of its entries. The form of the set of such permutations depends on the character of the degeneracy of the spectrum of ρ.

Representation (2.2) makes the description of some topological properties of the (N^2-1)-dimensional space $\mathcal{M}$ easier [24, 25]. We introduce the following notation. We write $T^N = (S^1)^N = [U(1)]^N$ for the N-dimensional torus. Identifying points of $\mathcal{S}_N$ which have the same coordinates (but ordered in a different way) we obtain an asymmetric simplex $\tilde{\mathcal{S}}_N$. Equivalently, one can divide $\mathcal{S}_N$ into $N!$ identical simplexes and take any of them. The asymmetric simplex $\tilde{\mathcal{S}}_N$ can be decomposed in the following natural way:

$$\tilde{\mathcal{S}}_N = \bigcup_{k_1+\cdots+k_n=N} K_{k_1,\ldots,k_n} \tag{2.3}$$

where $n = 1, \ldots, N$ denotes the number of different coordinates of a given point of $\tilde{\mathcal{S}}_N$, k_1 the number of occurrences of the largest coordinate, k_2 the second largest etc. Observe that $K_{k_1,\ldots,k_n}$ is homeomorphic with the set G_n, where G_1 is a single point, G_2 a half-closed interval, G_3 an open triangle with one edge but without corners and, generally, G_n is an $(n-1)$-dimensional simplex with one $(n-2)$-dimensional hyperface without boundary (the latter is homeomorphic with an $(n-2)$-dimensional open simplex). There are N ordered eigenvalues: $E_1 \geqslant E_2 \geqslant \cdots \geqslant E_N$, and $N-1$ independent relation operators 'larger or equal', which makes altogether 2^{N-1} different possibilities. Thus, $\tilde{\mathcal{S}}_N$ consists of 2^{N-1} parts, out of which $\binom{N-1}{m-1}$ parts are homeomorphic with G_m, when m ranges from 1 to N. The decomposition of the asymmetric simplex $\tilde{\mathcal{S}}_N$ is illustrated in figure 1 for the simplest cases, $N = 2$, 3 and 4.

Let us denote the part of the space $\mathcal{M}$ related to the spectrum in $K_{k_1,\ldots,k_n}$ (n different eigenvalues; the largest eigenvalue has k_1 multiplicity, the second largest k_2 etc) by $\mathcal{M}_{k_1,\ldots,k_n}$. A mixed state ρ with this kind of the spectrum remains invariant under arbitrary unitary rotations performed in each of the k_i-dimensional subspaces of degeneracy. Therefore the unitary matrix B has a block diagonal structure with n blocks of size equal to $k_1, \ldots, k_n$ and

$$\mathcal{M}_{k_1,\ldots,k_n} \sim [U(N)/(U(k_1) \times \cdots \times U(k_n))] \times G_n \tag{2.4}$$

where $k_1 + \cdots + k_n = N$ and $k_i > 0$ for $i = 1, \ldots, n$. Thus $\mathcal{M}$ has the structure

$$\mathcal{M} \sim \bigcup_{k_1+\cdots+k_n=N} \mathcal{M}_{k_1,\ldots,k_n} \sim \bigcup_{k_1+\cdots+k_n=N} [U(N)/(U(k_1) \times \cdots \times U(k_n))] \times G_n \tag{2.5}$$

where the sum ranges over all partitions of N. The group of rotation matrices B equivalent to $\Gamma = U(k_1) \times U(k_2) \times \cdots \times U(k_n)$ is called the *stability group* of $U(N)$.

Table 1. Topological structure of the space of mixed quantum states for a fixed number of levels N. The group of unitary matrices of size N is denoted by $U(N)$ and the unit circle (one-dimensional torus $\sim U(1)$) by T, while G_n represents a part of an $(n-1)$-dimensional asymmetric simplex defined in the text. The dimension D of the component $\mathcal{M}_{k_1,\ldots,k_n}$ is equal to $D_1 + D_2$, where D_1 denotes the dimension of the quotient space $U(N)/\Gamma$, while $D_2 = n - 1$ is the dimension of the part of the eigenvalue simplex homeomorphic with G_n.

N	Label	Decomposition	Subspace	Part of the asymmetric simplex	Topological structure	Dimension $D = D_1 + D_2$
1	$\mathcal{M}_1$	1	E_1	point	$[U(1)/U(1)] \times G_1 = \{\rho_*\}$	$0 = 0 + 0$
2	$\mathcal{M}_{11}$	$1 + 1$	$E_1 > E_2$	line with left edge	$[U(2)/T^2] \times G_2$	$3 = 2 + 1$
	$\mathcal{M}_2$	2	$E_1 = E_2$	right edge	$[U(2)/U(2)] \times G_1 = \{\rho_*\}$	$0 = 0 + 0$
3	$\mathcal{M}_{111}$	$1 + 1 + 1$	$E_1 > E_2 > E_3$	triangle with base without corners	$[U(3)/T^3] \times G_3$	$8 = 6 + 2$
	$\mathcal{M}_{12}$	$1 + 2$	$E_1 > E_2 = E_3$	edges with lower corners	$[U(3)/(U(2) \times T)] \times G_2$	$5 = 4 + 1$
	$\mathcal{M}_{21}$	$2 + 1$	$E_1 = E_2 > E_3$			
	$\mathcal{M}_3$	3	$E_1 = E_2 = E_3$	upper corner	$[U(3)/U(3)] \times G_1 = \{\rho_*\}$	$0 = 0 + 0$
4	$\mathcal{M}_{1111}$	$1 + 1 + 1 + 1$	$E_1 > E_2 > E_3 > E_4$	interior of tetrahedron with bottom face	$[U(4)/T^4] \times G_4$	$15 = 12 + 3$
	$\mathcal{M}_{112}$	$1 + 1 + 2$	$E_1 > E_2 > E_3 = E_4$	faces without side edges	$[U(4)/(U(2) \times T^2)] \times G_3$	$12 = 10 + 2$
	$\mathcal{M}_{121}$	$1 + 2 + 1$	$E_1 > E_2 = E_3 > E_4$			
	$\mathcal{M}_{211}$	$2 + 1 + 1$	$E_1 = E_2 > E_3 > E_4$			
	$\mathcal{M}_{13}$	$1 + 3$	$E_1 > E_2 = E_3 = E_4$	edges with lower corners	$[U(4)/(U(3) \times T)] \times G_2$	$7 = 6 + 1$
	$\mathcal{M}_{31}$	$3 + 1$	$E_1 = E_2 = E_3 > E_4$			
	$\mathcal{M}_{22}$	$2 + 2$	$E_1 = E_2 > E_3 = E_4$		$[U(4)/(U(2) \times U(2))] \times G_2$	$9 = 8 + 1$
	$\mathcal{M}_4$	4	$E_1 = E_2 = E_3 = E_4$	upper corner	$[U(4)/U(4)] \times G_1 = \{\rho_*\}$	$0 = 0 + 0$

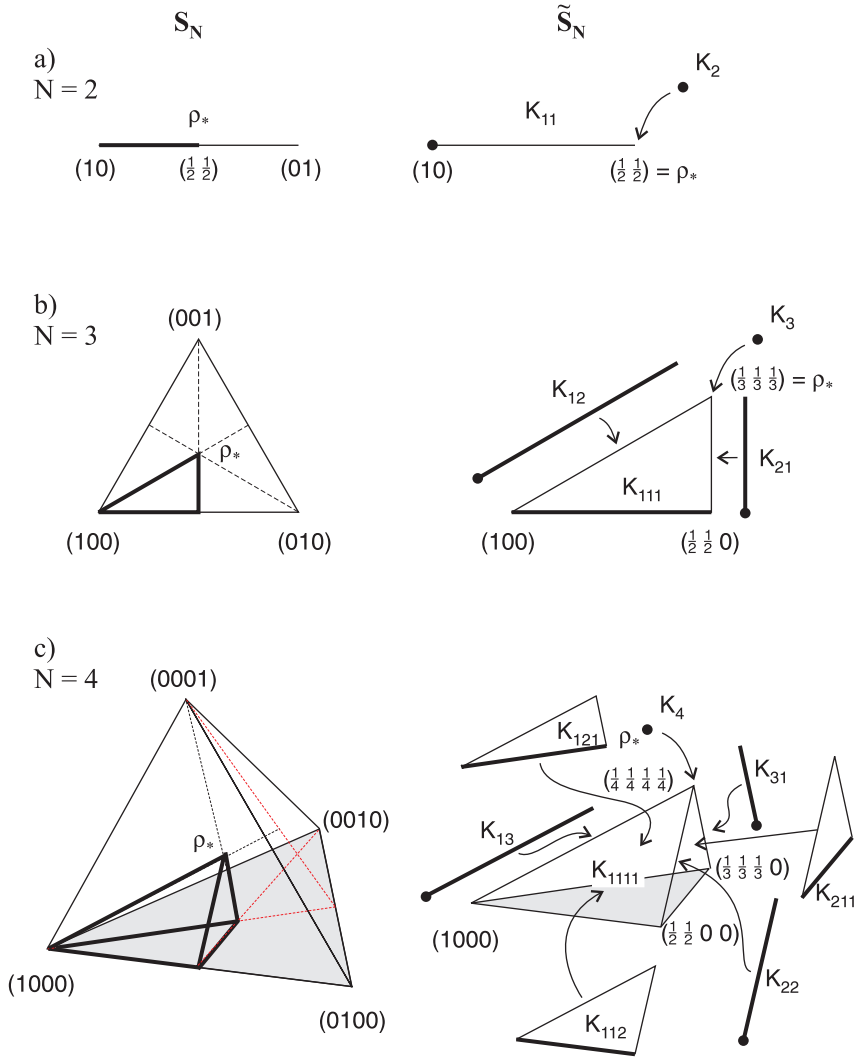

Figure 1. $(N-1)$-dimensional simplex $\mathcal{S}_N$ of diagonal density matrices of size N and its asymmetric part $\tilde{\mathcal{S}}_N$ for (a) $N=2$, (b) $N=3$ and (c) $N=4$. The simplex $\tilde{\mathcal{S}}_N$, enlarged on the right-hand side, can be decomposed into 2^{N-1} parts. N numbers in brackets denote coordinates in the original N-dimensional space of eigenvalues. Corners of $\tilde{\mathcal{S}}_N$ represent pure states (density matrices of rank one), edges—matrices of rank two and faces—matrices of rank two. Bold lines (grey faces) symbolize the boundary of $\tilde{\mathcal{S}}_N$.

For $N=2$ we have $\mathcal{M}_{1,1} \sim [U(2)/T^2] \times G_2 \sim S^2 \times G_2$ and $\mathcal{M}_2 \sim \{\rho_*\}$, so the space $\mathcal{M}$ has the topology of a two-dimensional ball—the Bloch sphere and its interior. This case and also cases $N=3,4$ are analysed in detail in table 1.

Note that the part $M_{1,\ldots,1}$ represents a generic, non-degenerate spectrum. In this case all elements of the spectrum of ρ are different and the stability group H is equivalent to an N-torus

$$\mathcal{M}_{1,\ldots,1} \sim [U(N)/T^N] \times G_N. \tag{2.6}$$

The above representation of generic states enables us to define a product measure in the space $\mathcal{M}$ of mixed quantum states. To this end, one can take the uniform (Haar) measure

on $U(N)$ and a certain measure on the simplex $\mathcal{S}_N$ [26, 27]. The coordinates of a point on the simplex may be generated [28] by squared moduli of components of a random orthogonal (unitary) matrix [29][4].

The other $2^{N-1}-1$ parts of $\mathcal{M}$ represent various kinds of degeneracy and have measure zero. The number of non-homeomorphic parts is equal to the number $P(N)$ of different representations of the number N as the sum of positive natural numbers. Thus $P(N)$ gives the number of different topological structures present in the space $\mathcal{M}$. For $N = 1, 2, \ldots, 10$ the number $P(N)$ is equal to 1, 2, 3, 5, 7, 11, 15, 22, 30 and 42, while for larger N it is described by the asymptotic Hardy–Ramanujan formula [30], $P(N) \sim \exp\left(\pi\sqrt{2N/3}\right)/4\sqrt{3}N$.

In the extreme case of N-fold degeneracy, $E_i \equiv 1/N$, the subspace $\mathcal{M}_N \sim [U(N)/(U(N) \times T^0)] \times G_1 \sim G_1$, so it degenerates to a single point. This distinguishes the maximally mixed state $\rho_* := \boldsymbol{I}/N$, which will play a crucial role in subsequent considerations. For the manifold of pure states $n = 2$ and $k_1 = 1, k_2 = N-1$ (since $E_1 = 1$, $E_2 = \cdots = E_N = 0$) and so $\mathcal{P} \sim [U(N)/(U(N-1) \times U(1))] \times (1, 0, \ldots, 0) \sim \mathbb{C}P^{N-1}$. In the case $N = 2$ it can be identified with the Bloch sphere S^2.

On the other hand, it is well known that $\mathcal{M}$ itself has the structure of a simplex with the boundary contained in the hypersurface $\det\rho = 0$, with rank one matrices (pure states—$\mathcal{P}$) as 'corners', rank two as 'edges' etc, and with the point ρ_* 'in the middle' (see [31, 32] for a formal statement and [33] for a nice intuitive discussion).

Let us mention in passing that the quotient space appearing in (2.4)

$$\mathbb{F} := \frac{U(N)}{U(k_1) \times U(k_2) \times \cdots \times U(k_n)} \tag{2.7}$$

is called a *complex flag manifold*, and in a special case

$$\mathrm{Gr}(k, N) := \frac{U(N)}{U(k) \times U(N-k)} \tag{2.8}$$

a *Grassman manifold*. For a fuller discussion of the topological structure of $\mathcal{M}$ (especially for $N = 4$) we refer the reader to [24].

2.2. Metric properties

The density matrix of a pure state $\rho_\psi = |\psi\rangle\langle\psi|$ may be represented in a suitable basis by a matrix with the first element equal to unity and all others equal to zero. Due to this simple form it is straightforward to compute the standard distances between ρ_ψ and ρ_* directly from the definitions recalled in section 1. Results do depend on the dimension N, but are independent of the pure state $|\psi\rangle$, namely

$$D_{\mathrm{tr}}(\rho_\psi, \rho_*) = 2 - \frac{2}{N} \qquad D_{\mathrm{HS}}(\rho_\psi, \rho_*) = \sqrt{1 - \frac{1}{N}} \qquad D_{\mathrm{Bures}}(\rho_\psi, \rho_*) = \sqrt{2 - \frac{2}{\sqrt{N}}}. \tag{2.9}$$

In the sense of the trace, the Hilbert–Schmidt or the Bures metric the $2(N-1)$-dimensional space of pure states $\mathcal{P}$ may be therefore considered as a part of the (N^2-1)-dimensional sphere centred at ρ_* of radius r depending on N and on the metric used. From the point of view of these standard metrics, no pure state on $\mathcal{P}$ is distinguished; all of them are equivalent. It is easy to show that the distance of any mixed state from ρ_* is smaller than r, in the sense of each of the standard metrics. Thus the space of mixed states $\mathcal{M}$ lies inside the sphere S^{N^2-2}

[4] In this paper a misprint occurred in the algorithm for generating random matrices typical of CUE. The corrected version (indices in the appendix B changed according to $r \to r+1$) can be found in *LANL preprint* chao-dyn/9707006.

embedded in $\mathbb{R}^{N^2-1}$, although, as discussed above, its topology (for $N > 2$) is much more complicated than the topology of the (N^2-1)-dimensional disc.

The degree of mixture of any state may be measured, for example by the *von Neumann entropy* $S = -\mathrm{Tr}\rho \ln \rho = -\sum_{i=1}^{N} E_i \ln(E_i)$. It varies from zero (pure states) to $\ln N$ (the maximally mixed state ρ_*). Let us briefly discuss a simple kicked dynamics, generated by a Hamiltonian represented by a Hermitian matrix H of size N. It maps a state ρ into

$$\rho' = \mathrm{e}^{\mathrm{i}H} \rho \mathrm{e}^{-\mathrm{i}H} \tag{2.10}$$

where the kicking period is set to unity.

Such a unitary quantum map does not change the eigenvalues of ρ, so the von Neumann entropy is conserved. In particular, any pure state is mapped by (2.10) into a pure state. Any mixed state ρ, which commutes with H, is not affected by this dynamics. Assume the Hamiltonian H to be generic, in the sense that its N eigenvalues are different. Then its invariant states form an $(N-1)$-dimensional subspace $\mathcal{I}_{\mathrm{H}} \subset M$, topologically equivalent to $\mathcal{S}_N$. In the generic case of a non-degenerate Hamiltonian it contains only N pure states: the eigenstates of H. Note that the invariant subspace $\mathcal{I}_{\mathrm{H}}$ always contains ρ_*.

Moreover, the standard distances between two states are conserved under the action of a unitary dynamics, i.e.

$$D_s(\rho_1, \rho_2) = D_s(\rho_1', \rho_2') \tag{2.11}$$

where D_s denotes one of the distances: D_{tr}, D_{HS} or D_{Bures}. Therefore, the unitary dynamics given by (2.10) can be considered as a generalized rotation in the (N^2-1)-dimensional space $\mathcal{M}$, around the $(N-1)$-dimensional 'hyperaxis' $\mathcal{I}_{\mathrm{H}}$, which is topologically equivalent to the simplex S^{N-1}. In the simplest case, $N = 2$, it is just a standard rotation of the Bloch ball around the axis determined by H. For example, if $H = \alpha J_z$, where J_z is the third component of the angular momentum operator J, it is just the rotation by angle α around the z axis joining both poles of the Bloch sphere. The set $\mathcal{I}_{\mathrm{H}}$ of states invariant with respect to this dynamics consists of all states diagonal in the basis of J_z: the mixed states with $\mathrm{diag}(\rho) = \{a, 1-a\}$ ($a \in (0, 1)$) and two pure states, $|1/2, 1/2\rangle$ for $a = 1$, and $|1/2, -1/2\rangle$ for $a = 0$.

3. Monge distance between quantum states

3.1. Monge transport problem and the Monge–Kantorovich distance

The original Monge problem, formulated in 1781 [34], emerged from studying the most efficient way of transporting soil [35].

Split two equally large volumes into infinitely small particles and then associate them with each other so that the sum of products of these paths of the particles over the volume is least. Along which paths must the particles be transported and what is the smallest transportation cost?

Consider two probability densities Q_1 and Q_2 defined in an open set $\Omega \subset R^n$, i.e. $Q_i \geqslant 0$ and $\int_\Omega Q_i(x)\, \mathrm{d}^n x = 1$ for $i = 1, 2$. Let V_1 and V_2, determined by Q_i, describe the initial and the final location of 'soil': $V_i = \{(x, y) \in \Omega \times R^+ : 0 \leqslant y \leqslant Q_i(x)\}$. The integral $\int_{V_i} \mathrm{d}^n x\, \mathrm{d}y$ is equal to unity due to normalization of Q_i. Consider C^1 one-to-one maps $T : \Omega \to \Omega$, which generate volume preserving transformations V_1 into V_2, i.e.

$$Q_1(x) = Q_2(Tx) \left| T'(x) \right| \tag{3.1}$$

for all $x \in \Omega$, where $T'(x)$ denotes the Jacobian of the map T at point x. We shall look for a transformation giving the minimal displacement integral and define the *Monge distance* [35,36]

$$D_{\mathrm{M}}(Q_1, Q_2) := \inf \int_\Omega |x - T(x)| Q_1(x)\, \mathrm{d}^n x \tag{3.2}$$

where the infimum is taken over all T as above. If the optimal transformation T_{M} exists, it is called a *Monge plan*. Note that in this formulation of the problem the 'vertical' component of the soil movement is neglected. The problem of the existence of such a transformation was solved by Sudakov [37], who proved that a Monge plan exists for Q_1, Q_2 smooth enough (see also [38]). The above definition can be extended to an arbitrary metric space (Ω, d) endowed with a Borel measure m. In this case one should put $d(x, T(x))$ instead of $|x - T(x)|$ and $\mathrm{d}m(x)$ instead of $\mathrm{d}^n x$ in formula (3.2), and take the infimum over all one-to-one and continuous $T : \Omega \to \Omega$ fulfilling $\int_A Q_1 \,\mathrm{d}m = \int_{T^{-1}(A)} Q_2 \,\mathrm{d}m$ for each Borel set $A \subset \Omega$. In fact we can also measure the Monge distance between two arbitrary probability measures in a metric space (Ω, d). For μ, ν probability measures on (Ω, d) we put

$$D_{\mathrm{M}}(\mu, \nu) := \inf \int_{\Omega} \mathrm{d}(x, T(x)) \,\mathrm{d}\mu\,(x) \tag{3.3}$$

where the infimum is taken over all one-to-one and continuous $T : \Omega \to \Omega$ such that $\mu(A) = \nu(T^{-1}(A))$ for each Borel set $A \subset \Omega$. To avoid the problem of the existence of a Monge plan Kantorovich [39,40] introduced in the 1940s the 'weak' version of the original Monge mass allocation problem and proved his famous variational principle (see proposition 1). For this and other interesting generalizations of the Monge problem consult the monographs by Rachev and Rüschendorf [36,41].

In some cases one can find the Monge distance analytically. For the one-dimensional case, $\Omega = \mathbb{R}$, the Monge distance can be expressed explicitly with the help of distribution functions $F_i(x) = \int_{-\infty}^{x} Q_i(t) \,\mathrm{d}t$, $i = 1, 2$. Salvemini obtained the following solution of the problem [43]:

$$D_{\mathrm{M}}(Q_1, Q_2) = \int_{-\infty}^{+\infty} |F_1(x) - F_2(x)| \,\mathrm{d}x. \tag{3.4}$$

Several two-dimensional problems with some kind of symmetry can be reduced to one-dimensional problems, solved by (3.4). In the general case one can estimate the Monge distance numerically [44], relying on algorithms for solving the transport problem, often discussed in handbooks of linear programming [45].

According to definition (3.2), taking an arbitrary map T which fulfils (3.1), we obtain an *upper bound* for the Monge distance D_{M}. Another two methods of estimating the Monge distance are valid for a compact metric space (Ω, d) equipped with a finite measure m. The first method may be used to obtain lower bounds for D_{M}. It is based on the proposition proved by Kantorovich in the 1940s [39,40] (see also [36,38,41,42]).

Proposition 1 (Variational formula for the Monge–Kantorovich metric).

$$D_{\mathrm{M}}(Q_1, Q_2) = \max \left| \int_{\Omega} f(x)\big(Q_1(x) - Q_2(x)\big) \,\mathrm{d}m\,(x) \right| \tag{3.5}$$

where the supremum is taken over all f fulfilling the condition $|f(x) - f(y)| \leqslant d(x, y)$ for all $x, y \in \Omega$ (weak contractions).

To obtain another *upper bound* for D_{M} we may apply the following simple estimate:

Proposition 2.

$$D_{\mathrm{M}}(Q_1, Q_2) \leqslant \frac{\Delta}{2} D_{L_1}(Q_1, Q_2) \tag{3.6}$$

where $D_{L_1}(Q_1, Q_2) = \int_{\Omega} |Q_1(x) - Q_2(x)| \,\mathrm{d}m\,(x)$ and $\Delta = \mathrm{diam}(\Omega)$.

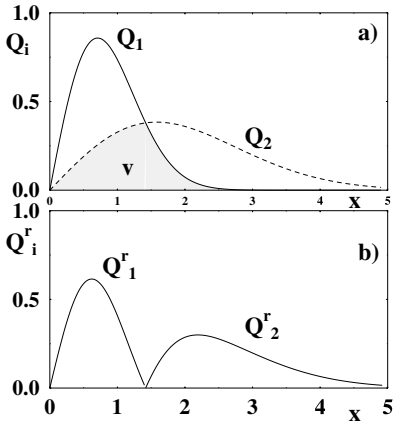

Figure 2. Estimation of the Monge distance between two overlapping distributions Q_1 and Q_2 (a) by the distance between the reduced distributions $Q_i^r(x) = Q_i(x) - V(x)$ (b), where $V(x)$ denotes the overlap.

The intuitive explanation of this fact is the following. Let v be the volume of the 'overlap' of the probability distributions Q_1 and Q_2; i.e. $v = \int_\Omega V(x)\,\mathrm{d}m\,(x)$, where $V = \min\{Q_1, Q_2\}$. Then $D_{\mathrm{M}}(Q_1, Q_2) \leqslant (1 - v)\Delta$, because the number $(1 - v)$ represents the part of the distribution to be moved and the largest possible classical distance on Ω is smaller than or equal to Δ. Moreover, $D_{L_1}(Q_1, Q_2) = 2(1 - v)$, which proves the assertion. Although figure 2 presents the corresponding picture for the simplest, one-dimensional case, proposition 2 is valid for an arbitrary metric space. For the formal proof see appendix A.

3.2. The Monge distance—harmonic oscillator coherent states

In [20] we defined a *'classical'* distance between two quantum states ρ_1 and ρ_2 via the Monge distance between the corresponding Husimi distributions H_{ρ_1} and H_{ρ_2}:

$$D_{\mathrm{M}}(\rho_1, \rho_2) := D_{\mathrm{M}}\left(H_{\rho_1}, H_{\rho_2}\right) \tag{3.7}$$

where H_{ρ_i} are given by formula (1.9). Observe that the family of harmonic oscillator coherent states $|\alpha\rangle$, parametrized by a complex number α, is implicitly present in this definition.

The Monge distance satisfies the *semiclassical property*: the distance between any two Glauber coherent states, represented by Gaussian Husimi distributions localized at points a_1 and a_2, is equal to the classical distance $|a_1 - a_2|$ in the complex plane [20].

3.3. The Monge distance—general case and basic properties

The above construction, originally performed for the complex plane with the help of the harmonic oscillator coherent states, may be extended to arbitrary generalized coherent states of Perelomov [46] defined on a compact classical phase space. Let G be a compact Lie group, $G \ni g \to R_g \in \mathcal{H}$ its irreducible unitary representation in the Hilbert space $\mathcal{H}$ and Υ the subgroup of G which consists of all elements $y \in G$ leaving the reference state $|\kappa\rangle \in \mathcal{P}$ invariant (i.e. $R_y|\kappa\rangle \sim |\kappa\rangle$). Define $\Omega = G/\Upsilon$ and $|\eta\rangle = R_\eta|\kappa\rangle$ for $[\eta] \in G/\Upsilon$. Note that $|1\rangle = |\kappa\rangle$, where 1 is the group G unit. Consider a family of the *generalized coherent states* $\Omega \ni \eta \to |\eta\rangle \in \mathcal{P}$. It satisfies the identity resolution $\int_\Omega |\eta\rangle\langle\eta|\,\mathrm{d}m\,(\eta) = \boldsymbol{I}/\dim\mathcal{H}$, where m is the natural (translation invariant) measure on the Riemannian manifold (Ω, d) normalized by the condition $m(\Omega) = 1$, and d is the Riemannian metric on Ω. Let us denote by $\mathcal{C}$ the manifold of all quantum coherent states, isomorphic to Ω, and embedded in the space of all pure states $\mathcal{P}$. Note that $\langle\eta|\eta\rangle \equiv 1$.

For the $SU(k)$ coherent states the space $\Omega \sim \mathcal{C}$ is isomorphic to $\mathbb{C}P^{k-1}$ and m is the natural Riemannian measure on Ω. Obviously, the dimension of the Hilbert space $\mathcal{H}_N$ carrying the representation of the group is equal to $N \geqslant k$, and if $N = k$ all pure states are $SU(k)$ coherent, and $\mathcal{C} = \mathcal{P}$. For example, in the case of $SU(2)$ vector coherent states the corresponding classical phase space is the sphere $S^2 \simeq \mathbb{C}P^1$ [46]. In the simplest case $N = 2$ (or $j = 1/2$) pure states are located at the Bloch sphere and are coherent.

Any quantum state $\rho \in \mathcal{M}$ may be represented by a generalized Husimi distribution $H_\rho : \Omega \to \mathbb{R}^+$ defined by

$$H_\rho(\eta) := N \cdot \langle \eta|\rho|\eta\rangle \tag{3.8}$$

for $\eta \in \Omega$, which satisfies

$$\int_\Omega H_\rho(\eta)\, \mathrm{d}m\,(\eta) = 1. \tag{3.9}$$

In particular, for a pure state $\rho = |\vartheta\rangle\langle\vartheta|$ ($|\vartheta\rangle \in \mathcal{P}$) and $\eta \in \Omega$ we have

$$H_{|\vartheta\rangle\langle\vartheta|}(\eta) := N|\langle\vartheta|\eta\rangle|^2. \tag{3.10}$$

In the following we shall assume that for coherent states $|\vartheta\rangle \in \mathcal{C}$ ($\vartheta \in \Omega$) the densities $H_{|\vartheta\rangle\langle\vartheta|}$ tend weakly to the Dirac-delta measure δ_ϑ in the *semiclassical limit*, i.e. when the dimension of the Hilbert space carrying the representation tends to infinity.

The Monge distance for the Hilbert space $\mathcal{H}_N$, the classical phase space (Ω, d) and the corresponding family of generalized coherent states $|\eta\rangle$ is then defined by solving the Monge problem in Ω, in full analogy with (3.7):

$$D_{\mathrm{M}}(\rho_1, \rho_2) := D_{\mathrm{M}}\left(H_{\rho_1}, H_{\rho_2}\right). \tag{3.11}$$

The distance $d(\eta, T(\eta))$ between the initial point η and its image $T(\eta)$ with respect to the Monge plan has to be computed along the geodesic lines on the Riemannian manifold Ω.

For compact spaces Ω the semiclassical condition (1.8) for the distance between two coherent states becomes weaker:

Property A (Semiclassical condition). Let $\eta_1, \eta_2 \in \Omega$. Then

$$D_{\mathrm{M}}(|\eta_1\rangle, |\eta_2\rangle) \leqslant d(\eta_1, \eta_2) \tag{3.12}$$

and

$$D_{\mathrm{M}}(|\eta_1\rangle, |\eta_2\rangle) \to d(\eta_1, \eta_2) \qquad \text{(in the semiclassical limit)} \tag{3.13}$$

where d represents the Riemannian distance between two points in Ω.

To demonstrate (3.12) it suffices to take for the transformation T in (3.2) the group translation $\eta_2 * {\eta_1}^{-1}$ (e.g. the respective rotation of the sphere S^2 in the case of $SU(2)$ coherent states). However, this transformation does not necessarily provide the optimal Monge plan. As we shall show in the following section, this is so for the sphere and the $SU(2)$ coherent states. On the other hand, in the semiclassical limit (for $SU(2)$ coherent states $j \to \infty$), the inequality in (3.12) converts into the equality, in full analogy to the property (1.8), valid for the complex plane and the harmonic oscillator coherent states. This follows from the fact that the Monge–Kantorovich metric generates the weak topology in the space of all probability measures on Ω, and the densities $H_{|\eta_i\rangle\langle\eta_i|}$ tend weakly to the Dirac delta δ_{η_i} in the semiclassical limit, for $i = 1, 2$.

The Monge distance defined above is invariant under the action of group translations, namely:

Property B (Invariance). Let $\alpha, \beta \in G$ and $\rho_1, \rho_2 \in \mathcal{M}$. Then

$$D_{\mathrm{M}}(R_\beta{}^{-1}\rho_1 R_\beta, R_\beta{}^{-1}\rho_2 R_\beta) = D_{\mathrm{M}}(\rho_1, \rho_2). \tag{3.14}$$

Particularly,

$$D_{\mathrm{M}}(|\alpha\rangle, |\beta\rangle) = D_{\mathrm{M}}(|\beta^{-1}\alpha\rangle, |1\rangle) \tag{3.15}$$

where 1 is the group G unit.

The above formulae follow from the definition of the Monge distance (3.3), and from the fact that both the measure m and the metric d are translation invariant.

3.4. Relation to other distances

Let $\rho_1, \rho_2 \in \mathcal{M}$. We start by recalling the variational formula for the trace distance (see for instance [47]).

Proposition 3 (Variational formula for D_{tr}).

$$D_{\mathrm{tr}}(\rho_1, \rho_2) = \sup_{\|A\| \leqslant 1} |\operatorname{tr} A(\rho_1 - \rho_2)| \tag{3.16}$$

where the supremum is taken over all Hermitian matrices A such that $\|A\| \leqslant 1$, and the supremum norm reads

$$\|A\| = \sup\{\|Ax\| : x \in \mathcal{H}_{\mathcal{N}}, \|x\| \leqslant 1\}. \tag{3.17}$$

Applying proposition 1 we can prove an analogous formula for the Monge distance.

Proposition 4 (Variational formula for D_{M}).

$$D_{\mathrm{M}}(\rho_1, \rho_2) = \max_{L(A) \leqslant 1} |\operatorname{tr} A(\rho_1 - \rho_2)| \tag{3.18}$$

where the maximum is taken over all Hermitian matrices A with $L(A) \leqslant 1$, and

$$L(A) = \inf \Bigg\{ c : \textit{there exists a } c\textit{-Lipschitzian function } f : \Omega \to \mathbb{R} \textit{ such that } A = \int_\Omega f(\eta)|\eta\rangle\langle\eta| \, \mathrm{d}m(\eta) \Bigg\}. \tag{3.19}$$

For the proof see appendix B. This proposition has a simple physical interpretation. It says that *the Monge distance between two quantum states is equal to the maximal value of the difference between the expectation values (in these states) of observables (Hermitian operators), some of whose P-representations are weak contractions*. Recently, Rieffel [48] considered the class of metrics on state spaces which are generated by Lipschitz seminorms. If Ω is compact, then one can show that the Monge metric D_{M} belongs to this class.

From propositions 3 and 4 we can also easily deduce proposition 2. Using proposition 2 and the Hölder inequality for the trace (see [47]) one can prove the following inequalities:

$$\frac{2}{\Delta} D_{\mathrm{M}} \leqslant D_{L_1} \leqslant N \cdot D_{\mathrm{HS}} \leqslant N \cdot D_{\mathrm{tr}} \tag{3.20}$$

where Δ is the diameter of Ω and $N = \dim \mathcal{H}_{\mathcal{N}}$. On the other hand from the fact that the Monge–Kantorovich metric generates the weak topology in the space of probability measures on Ω, it follows that $D_{\mathrm{M}}(\rho_1, \rho_2) \to 0$ implies $D_{\mathrm{HS}}(\rho_1, \rho_2) \to 0$ for every $\rho_1, \rho_2 \in \mathcal{M}$. Thus the Monge metric D_{M} and the Hilbert–Schmidt metric D_{HS} generate the same topology in the space of mixed states $\mathcal{M}$.

Let us emphasize here a crucial difference between our 'classical' Monge distance and the standard distances in the space of quantum states. Given any two quantum states represented by the density matrices ρ_1 and ρ_2, one may directly compute the trace, the Hilbert–Schmidt or the Bures distance between them. On the other hand, the classical distance is defined by specifying the set of generalized coherent states in the Hilbert space. In other words, one needs to choose a classical phase space with respect to which the Monge distance is defined. Take for example two density operators of size $N = 3$. The distance $D_{\mathrm{M}}(\rho_1, \rho_2)$ computed with respect to the $SU(2)$ coherent states and, say, with respect to the $SU(3)$ coherent states can be different. The simplest case of the $SU(2)$ coherent states corresponding to classical dynamics on the sphere is discussed in the following section.

4. Monge metric on the sphere

4.1. Spin coherent state representation

Let us consider a classical area preserving map on the unit sphere $\Theta : S^2 \to S^2$ and a corresponding quantum map U acting in an N-dimensional Hilbert space $\mathcal{H}_N$. A link between classical and quantum mechanics can be established via a family of spin coherent states $|\vartheta, \varphi\rangle \in \mathcal{H}$ localized at points (ϑ, φ) of the sphere $\mathbb{C}P^1 = S^2$. The vector coherent states were introduced by Radcliffe [49] and Arecchi *et al* [50] and their various properties are often analysed in the literature (see e.g. [51, 52]). They are related to the $SU(2)$ algebra of the components of the angular momentum operator $J = \{J_x, J_y, J_z\}$, and provide an example of the general group theoretic construction of Perelomov [46] (see section 3.3).

Let us choose a reference state $|\kappa\rangle$, usually taken as the maximal eigenstate $|j, j\rangle$ of the component J_z acting on $\mathcal{H}_N$, $N = 2j + 1$, $j = 1/2, 1, 3/2, \ldots$. This state, pointing toward the 'north pole' of the sphere, enjoys the minimal uncertainty equal to j. Then, the vector coherent state is defined by the Wigner rotation matrix $R_{\vartheta,\varphi}$

$$|\vartheta, \varphi\rangle = R_{\vartheta,\varphi}|\kappa\rangle = (1 + |\gamma|^2)^{-j} \mathrm{e}^{\gamma J_-}|j, j\rangle \tag{4.1}$$

where $R_{\vartheta,\varphi} = \exp\left[\mathrm{i}\vartheta\left(\cos\varphi J_x - \sin\varphi J_y\right)\right]$, $J_- = J_x - \mathrm{i}J_y$ and $\gamma = \tan(\vartheta/2)\mathrm{e}^{\mathrm{i}\varphi}$, for $(\vartheta, \varphi) \in S^2$ (we use the spherical coordinates).

We obtain the coherent state identity resolution in the form

$$\int_{S^2} |\vartheta, \varphi\rangle\langle\vartheta, \varphi| \, \mathrm{d}\mu\,(\vartheta, \varphi) = \boldsymbol{I}/(2j + 1) \tag{4.2}$$

where the Riemannian measure $\mathrm{d}\mu\,(\vartheta, \varphi) = (\sin\vartheta/4\pi)\,\mathrm{d}\vartheta\,\mathrm{d}\varphi$ does not depend on the quantum number j.

Expansion of a coherent state in the common eigenbasis of J_z and J^2 in $\mathcal{H}_N$: $|j, m\rangle$, $m = -j, \ldots, +j$ reads

$$|\vartheta, \varphi\rangle = \sum_{m=-j}^{m=j} \sin^{j-m}(\vartheta/2)\cos^{j+m}(\vartheta/2)\exp\left(\mathrm{i}(j - m)\varphi\right)\left[\binom{2j}{j-m}\right]^{1/2}|j, m\rangle. \tag{4.3}$$

The infinite 'basis' formed in the Hilbert space by the coherent states is overcomplete. Two different $SU(2)$ coherent states overlap unless they are directed into two antipodal points on the sphere. Expanding the coherent states in the basis of $\mathcal{H}_N$ as in (4.3) we calculate their overlap

$$|\langle\vartheta', \varphi'|\vartheta, \varphi\rangle|^2 = \cos^{4j}(\Xi/2) \tag{4.4}$$

where Ξ is the angle between two vectors on S^2 related to the coherent states $|\vartheta, \varphi\rangle$ and $|\vartheta', \varphi'\rangle$, and for $j = 1/2$ it is twice the geodesic distance (1.7). Thus, we have

$$H_{|\vartheta,\varphi\rangle\langle\vartheta,\varphi|}(\vartheta', \varphi') = (2j + 1)\cos^{4j}(\Xi/2). \tag{4.5}$$

This formula guarantees that the respective Husimi distribution of an arbitrary spin coherent state tends to the Dirac δ-function in the semiclassical limit $j \to \infty$.

To calculate the Monge distance between two arbitrary density matrices ρ_1 and ρ_2 of size N one uses the $N = (2j+1)$-dimensional representation of the spin coherent states $|\vartheta, \varphi\rangle$ (to simplify the notation we did not label them by the quantum number j). Next, one computes the generalized Husimi representations for both states

$$H_{\rho_i}(\vartheta, \varphi) := N \cdot \langle \vartheta, \varphi | \rho_i | \vartheta, \varphi \rangle \tag{4.6}$$

and solves the Monge problem on the sphere for these distributions. Increasing the parameter j (quantum number) one may analyse the semiclassical properties of the Monge distance.

It is sometimes useful to use the stereographical projection of the sphere S^2 onto the complex plane. The Husimi representation of any state ρ becomes then the function of a complex parameter z. It is easy to see that for any pure state $|\psi\rangle \in \mathcal{P}$ the corresponding Husimi representation is given by a polynomial of $(N-1)$ order: $W_\psi(z) = z^{N-1} + \sum_{i=0}^{N-2} c_l z^l = 0$ with arbitrary complex coefficients c_i. This fact provides an alternative explanation of the equality $\mathcal{P} = \mathbb{C}P^{N-1}$. Thus, every pure state can be uniquely determined by the position of the $(N-1)$ zeros of W_ψ on the complex plane (or, equivalently, by zeros of $H_{|\psi\rangle}$ on the sphere). Such *stellar* representation of pure states is due to Majorana [53] and it found several applications in the investigation of quantum dynamics [54–56]. In general, the zeros of the Husimi representation may be degenerate. This is just the case for the coherent states: the Husimi function of the state $|\vartheta, \varphi\rangle$ is equal to zero only at the antipodal point and the $(N-1)$-fold degeneracy occurs. The stellar representation is used in section 6 to define a simplified Monge metric in the space of pure quantum states.

4.2. Monge distance between some symmetrical states

Consider two quantum states, whose Husimi distributions are invariant with respect to the horizontal rotation. Using proposition 4 one may find the Monge distance between the two states with the help of the Salvemini formula (3.4)

Proposition 5. *Let $\rho_1, \rho_2 \in \mathcal{M}$ fulfil $H_{\rho_i}(\vartheta, \varphi) = \tilde{H}_{\rho_i}(\vartheta)$ for $(\vartheta, \varphi) \in S^2$. Consider the normalized one-dimensional functions $h_{\rho_i} : [0, \pi] \to \mathbb{R}^+$ given by $h_{\rho_i}(\vartheta) := \tilde{H}_{\rho_i}(\vartheta) \frac{1}{2} \sin\vartheta$ that satisfy $\int_0^\pi h_{\rho_i}(\vartheta)\, \mathrm{d}\vartheta = 1$ for $i = 1, 2$. Then*

$$D_{\mathrm{M}}(\rho_1, \rho_2) = \int_0^\pi \left| F_{\rho_1}(\vartheta) - F_{\rho_2}(\vartheta) \right| \mathrm{d}\vartheta \tag{4.7}$$

where the cumulative distributions read $F_{\rho_i}(\vartheta) = \int_0^\vartheta h_{\rho_i}(\psi)\, \mathrm{d}\psi$.

The proof is given in appendix C. We use this proposition in computing the Monge distance between two arbitrary eigenstates of the operator J_z (section 4.6.1) and the Monge distance of some of these eigenstates from the maximally mixed state (section 4.6.2).

The maximally mixed state $\rho_* = \boldsymbol{I}/N$ is represented by the uniform Husimi distribution on the sphere. Thus, $H_{\rho_*}(\vartheta, \varphi) = \tilde{H}_{\rho_*}(\vartheta) = 1$, $h_{\rho_*}(\vartheta) = \frac{1}{2}\sin\vartheta$ and $F_{\rho_*}(\vartheta) = \frac{1}{2}(1 - \cos\vartheta)$.

Furthermore, all the eigenstates of J_z, forming the basis $|j, m\rangle$, possess this symmetry, and according to (4.3) we obtain

$$h_{|j,m\rangle\langle j,m|}(\vartheta) = (2j+1) \begin{pmatrix} 2j \\ j-m \end{pmatrix} \sin^{2(j-m)+1}(\vartheta/2) \cos^{2(j+m)+1}(\vartheta/2). \tag{4.8}$$

The formula (4.7) enables us to compute the Monge distance between them.

We introduce the notation $\rho_+ = |j, j\rangle\langle j, j|$, $\rho_- = |j, -j\rangle\langle j, -j|$, and $\rho_a = a\rho_+ + (1-a)\rho_-$ for $a \in [0, 1]$ (for $N = 2$ these states are represented in figure 3). It follows

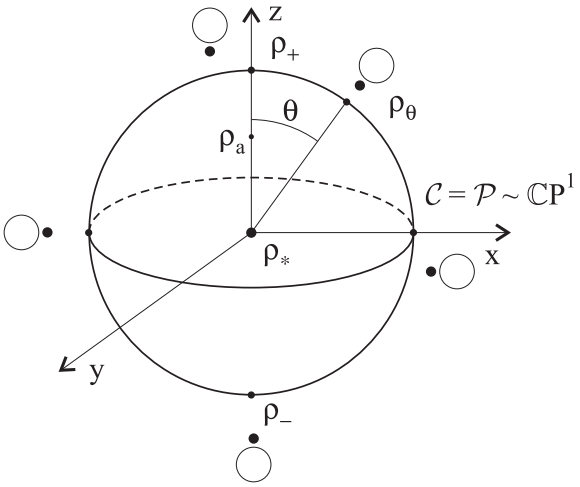

Figure 3. Quantum states, for which we calculate Monge distances, are denoted at the Bloch sphere corresponding to $j = 1/2$. Dots at small circles represent the positions of zeros of the Husimi function of the corresponding pure states.

from proposition 1 that $H_{\rho_a} = aH_{\rho_+} + (1-a)H_{\rho_-}$, and, consequently, $D_{\mathrm{M}}(\rho_+, \rho_a) = (1-a)D_{\mathrm{M}}(\rho_+, \rho_-)$, and $D_{\mathrm{M}}(\rho_a, \rho_-) = aD_{\mathrm{M}}(\rho_+, \rho_-)$.

In some cases we can reduce the two-dimensional problem to the Salvemini formula, even if it does not possess rotational symmetry.

Proposition 6. *Let* $\rho_1, \rho_2 \in \mathcal{M}$. *Define* $F_i : [0,\pi] \times [0,2\pi] \to [0,1]$ *by* $F_i(t,\varphi) = \frac{1}{2}\int_0^t H_{\rho_i}(\vartheta,\varphi)\sin\vartheta\,\mathrm{d}\vartheta$ *for* $t \in [0,\pi]$, $\varphi \in [0,2\pi]$, *and* $i = 1, 2$. *Assume that*

(1) $F_1(\pi,\varphi) = F_2(\pi,\varphi)$ *for all* $\varphi \in [0,2\pi]$,
(2) $F_1(t,\varphi) \geqslant F_2(t,\varphi)$ *for all* $t \in [0,\pi]$ *and* $\varphi \in [0,2\pi]$.

Then

$$D_{\mathrm{M}}(\rho_1,\rho_2) = \frac{1}{2\pi}\int_0^{2\pi}\int_0^{\pi}\big(F_1(t,\varphi) - F_2(t,\varphi)\big)\,\mathrm{d}t\,\mathrm{d}\varphi. \tag{4.9}$$

For the proof see appendix D. We use the above proposition for computing both the Monge distance between two arbitrary density matrices for $j = 1/2$ (section 4.3) and the Monge distance between two coherent states for arbitrary j (section 4.6.3).

4.3. Monge distances for $j = 1/2$

Let us start from the calculation of the Monge distance between the 'north pole' ρ_+ and a mixed state ρ_a parametrized by $a \in (0,1)$ (note that $\rho_* = \rho_{1/2}$ in this case). Computing the distribution functions we obtain $F_{\rho_a}(\vartheta) = (\sin^2\vartheta)(2a-1)/4 + (1-\cos\vartheta)/2$, while $F_{\rho_+}(\vartheta) = F_{\rho_{a=1}}(\vartheta)$. Elementary integration (4.7) gives the result $D_{\mathrm{M}}(\rho_+,\rho_a) = (1-a)\pi/4$. Substituting $a = 1/2$ for ρ_* or $a = 0$ for ρ_- we obtain two important special cases:

$$D_{\mathrm{M}}(\rho_+,\rho_-) = \pi/4 \qquad D_{\mathrm{M}}(\rho_+,\rho_*) = D_{\mathrm{M}}(\rho_-,\rho_*) = \pi/8. \tag{4.10}$$

These three states ρ_+, ρ_* and ρ_- lie on a metric line. This follows from the property of the distribution functions visible in figure 4. They do not intersect, and therefore the area between F_+ and F_- is equal to the sum of two figures: one enclosed between F_+ and F_*, and the other one enclosed between F_* and F_-. Note, however, that the distance $D_{\mathrm{M}}(\rho_+,\rho_-) \approx 0.785$ is much smaller than the classical distance between two poles on the sphere equal to π. Instead of rotating the distribution H_{ρ_+} by the angle π, the optimal Monge plan consists in moving south the 'sand' occupying the north pole, along each meridian. The difference between the two

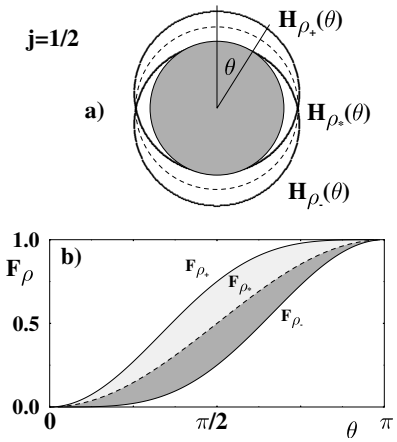

Figure 4. (*a*) Cross-section of the Husimi distribution $H_\rho(\vartheta)$ for ρ_+ (peaked at the top), for ρ_* (uniform) and for ρ_- (peaked at the bottom) plotted for $j = 1/2$. (*b*) The Monge distance between these states may be represented as the area between graphs of the corresponding distribution functions $F_{\rho_+}(\vartheta)$, $F_{\rho_*}(\vartheta)$ and $F_{\rho_-}(\vartheta)$.

transformations is so large only in this deep quantum regime, for which the distributions are very broad and strongly overlap. As demonstrated below, this effect vanishes in the semiclassical regime $j \to \infty$, where the semiclassical property (1.8) is recovered.

In the case $j = 1/2$ all pure states are coherent, so the Monge distance from ρ_* is the same for every pure state (as illustrated in figure 3). Thus, the manifold of pure states (the Bloch sphere) forms, in the sense of the Monge metric, the sphere S^2 of radius $R_1 = \pi/8$ centred at ρ_*. All mixed states are less localized than coherent and their distance to ρ_* is smaller than R_1. To see this note that every mixed state can be represented as a vector $\boldsymbol{v}$ in the unit ball. Using proposition 6 and some geometrical considerations one can find the Monge distance between any two mixed states ρ_1 and ρ_2. Representing them by Pauli matrices $\vec{\sigma}$ and vectors $\vec{v}_i$ in the Bloch ball of radius $1/2$, namely, $\rho_i = \rho_* + \vec{\sigma} \cdot \vec{v}_i$, we obtain [57]

$$D_{\mathrm{M}}(\rho_1, \rho_2) = \frac{\pi}{4}\, d(\vec{v}_1, \vec{v}_2) = \frac{\pi}{4}|\vec{v}_1 - \vec{v}_2| \tag{4.11}$$

where d denotes the Euclidean metric in $\mathbb{R}^3$. Consequently, for $j = 1/2$ the Monge distance induces the same geometry as that of the Bloch ball, as illustrated in figure 3.

4.4. Monge distances for $j = 1$

In an analogous way we treat the case $N = 3$. Obtained data

$$R_1 := D_{\mathrm{M}}(\rho_+, \rho_*) = D_{\mathrm{M}}(\rho_-, \rho_*) = 3\pi/16 \qquad D_{\mathrm{M}}(\rho_+, \rho_-) = 3\pi/8 \tag{4.12}$$

$$R_2 := D_{\mathrm{M}}(\rho_*, \rho_{|0\rangle}) = 1/6 \qquad D_{\mathrm{M}}(\rho_+, \rho_{|0\rangle}) = D_{\mathrm{M}}(\rho_-, \rho_{|0\rangle}) = 3\pi/16 \tag{4.13}$$

are based on the results derived in appendix E (see also section 4.5) and visualized in figure 5(*b*). Note that both triples $\{\rho_+, \rho_*, \rho_-\}$ and $\{\rho_+, \rho_{|0\rangle}, \rho_-\}$ lie on two different metric curves. Thus, in contrast to the case $j = 1/2$, the two states ρ_+ and ρ_- are connected by several different metric curves.

Now, consider a mixed state ρ_m represented in the canonical basis by a diagonal density matrix $\rho_m = \mathrm{diag}(a, b, c)$, where $a + b + c = 1$. Since $\{\rho_+, \rho_{|0\rangle}, \rho_-\}$ lie on a metric curve and their distributions are invariant with respect to the horizontal rotation, it is not difficult to

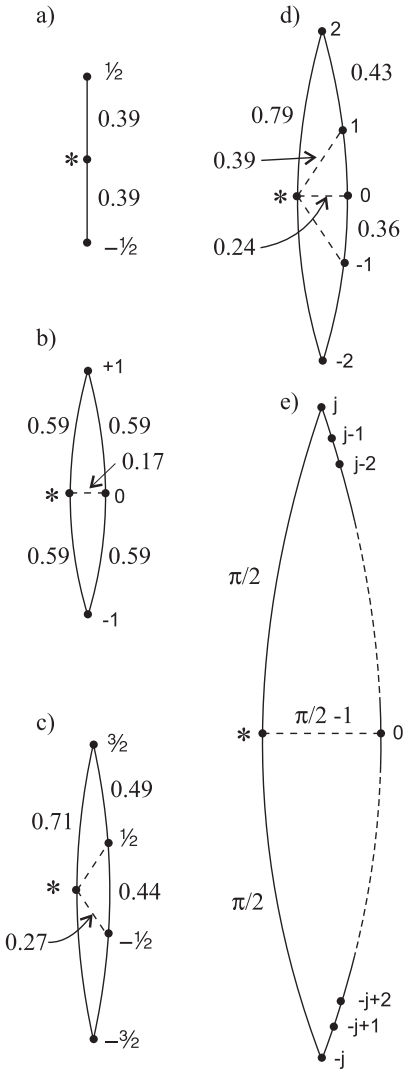

Figure 5. Schematic map showing the eigenstates $|j, m\rangle$ and the mixed state ρ_* for (*a*) $j = 1/2$, (*b*) $j = 1$, (*c*) $j = 3/2$, (*d*) $j = 2$ and (*e*) $j \to \infty$. The symbol $*$ labelling dots represents the maximally mixed state ρ_*, while numbers m denote pure states $|j, m\rangle$. Solid curves denote the metric curves, and the accompanying numbers represent the approximate Monge distance between the states.

calculate the Monge distance $D_{\mathrm{M}}(\rho_+, \rho_m)$ using proposition 5. The corresponding distribution functions do not cross, and so $D_{\mathrm{M}}(\rho_+, \rho_m) = bD_{\mathrm{M}}(\rho_+, \rho_{|0\rangle}) + cD_{\mathrm{M}}(\rho_+, \rho_-) = \frac{3\pi}{16}(2-b-2a)$. For comparison $D_{\mathrm{HS}}(\rho_+, \rho_m) = \sqrt{(1-a)^2 + b^2 + (1-a-b)^2}$, $D_{\mathrm{tr}}(\rho_+, \rho_m) = \sqrt{2(1-a)}$ and $D_{\mathrm{Bures}} = \sqrt{2(1-\sqrt{a})}$. This simple example shows that for $j = 1$ the Monge metric induces a non-trivial geometry, considerably different from geometries generated by any standard metric.

The Monge distance R_ψ between any pure state $|\psi\rangle$ and the mixed state ρ_* depends only on the angle χ between two zeros of the Husimi function located on the sphere. If the zeros are degenerate, $\chi = 0$, the state is coherent and $R_\psi = R_1$. The coherent states are as localized in the phase space as is allowed by the Heisenberg uncertainty relation. It is therefore intuitive to expect that out of all pure states the coherent states are the most distant from ρ_*. In the other extreme case, both zeros lie at the antipodal points, $\chi = \pi$, which corresponds to $\rho_{|0\rangle}$, and $R_\psi = R_2$. In this symmetrical case, the Husimi distribution is as delocalized as possible,

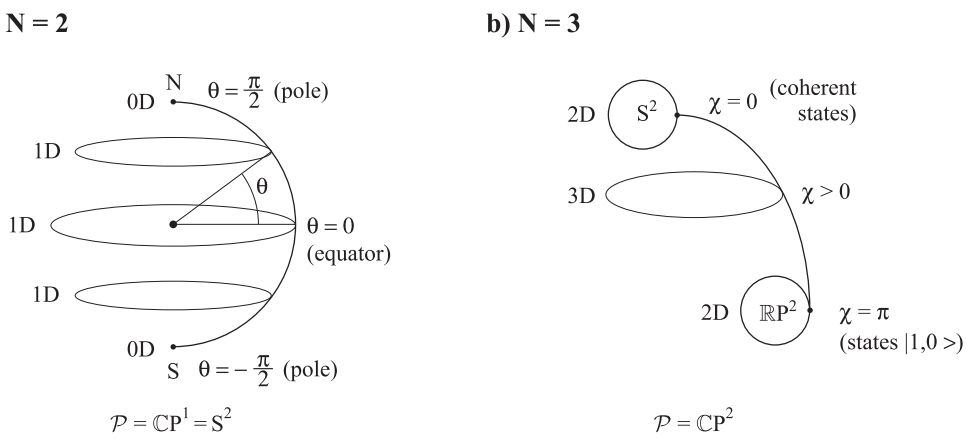

Figure 6. Foliation of the sphere along the Greenwich meridian (a), foliation of the four-dimensional space of the $N = 3$ pure states along the angle χ between the two zeros of the corresponding Husimi distribution (b). The poles correspond to the distinguished 2D submanifolds of $\mathbb{C}P^2$: the manifold S^2 of coherent states and the manifold $\mathbb{R}P^2$ of states equivalent to $|1, 0\rangle$.

and we conjecture that for every pure state its distance from ρ_* is larger than or equal to R_2.

Thus, considering the Monge distance from ρ_*, one obtains a foliation of the space of pure states $\mathcal{P} = \mathbb{C}P^2$, as shown in figure 6($b$). As a running parameter we may take the angle χ, which describes a pure state in the stellar representation. This foliation is singular, since the topology of the leaves depends on the angle. The angle $\chi = 0$ represents the sphere S^2 of coherent states ($\sim SO(3)/SO(2)$), intermediate angle represents a generic 3D manifold $\mathbb{R}P^3/\mathbb{Z}_2$ (a desymmetrized Stiefel manifold $\sim SO(3)/\mathbb{Z}_2$) of pure states of the same χ, while the limiting value $\chi = \pi$ denotes the $\mathbb{R}P^2$ ($\sim SO(3)/O(3)$) manifold of states rotationally equivalent to $\rho_{|0\rangle}$. Similar foliations of $\mathcal{P}$ discussed in another context may be found in Bacry [54] and in a recent paper by Barros and Sá [58]. For comparison in figure 6(a) we present the foliation of $\mathbb{C}P^1$ as regards the Monge distance from ρ_+.

Since it is hardly possible to provide a plot of $\mathcal{M}$ revealing all details of this non-trivial, eight-dimensional space of mixed states, we cannot expect too much from figure 7, which should be treated with a pinch of salt. As discussed in section 2, from the point of view of the standard metrics, the four-dimensional manifold of the pure states $\mathcal{P}$ is contained in the sphere S^7 centred at ρ_*. For the Monge metric one has $R_1 > R_2$, so we suggest illustrating $\mathcal{M}$ as an eight-dimensional full 'hyper-ellipsoid'. Pure states ρ_+ and ρ_- occupy its poles along the longest axis. The dashed vertical ellipse represents the space of all coherent states $\mathcal{C}$, which forms the sphere S^2 of radius R_1. The solid horizontal ellipse represents these pure states, which are closest to ρ_*. This subspace may be obtained from $|0\rangle\langle 0|$ by a three-dimensional rotation of coordinates; topologically it is a real projective space $\mathbb{R}P^2$. Although both ellipses do cross in the picture, the two manifolds do not have any common points, which is easily possible in the four-dimensional space $\mathcal{P}$. To simplify the identification of single pure states we added to the picture small circles with two dark dots, which indicate their stellar representations. In general, the states represented by points inside the hyper-ellipsoid are mixed. However, since $\mathcal{M}$ is only a part of the hyper-ellipsoid, not all points inside this figure represent existing mixed states.

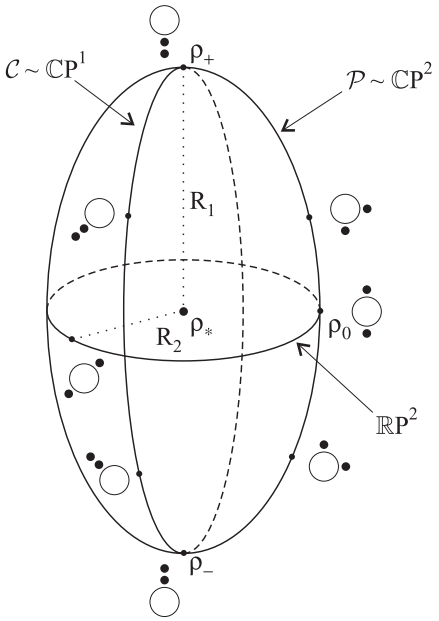

Figure 7. Sketch of the structure of the space of the mixed states $\mathcal{M}$ for $j = 1$ induced by the Monge metrics. The manifold of the coherent states $\mathcal{C} = S^2$ is represented by a circle of radius $R_1 = 3\pi/16 \sim 0.589$ centred at ρ_*. Pure states isomorphic to $\rho_{|0\rangle}$ are situated $R_2 = 1/6 \sim 0.166$ from ρ_*. Dots at smaller circles represent the positions of zeros z_1 and z_2, which determine each pure state in the stellar representation.

4.5. The cases $j = 3/2$ and $j = 2$

For $j = 3/2$ ($N = 4$) the results read in a simplified notation $D^{(N=4)}_{3/2,1/2} = D^{(N=4)}_{-1/2,-3/2} = 5\pi/32$, $D^{(N=4)}_{1/2,-1/2} = 9\pi/64$, $D^{(N=4)}_{3/2,*} = D^{(N=4)}_{-3/2,*} = 29\pi/128$ and $D^{(N=4)}_{1/2,*} = D^{(N=4)}_{-1/2,*} \simeq 0.2737$. For $j = 2$ ($N = 5$) one obtains $D^{(N=5)}_{2,1} = D^{(N=5)}_{-1,-2} = 35\pi/256$, $D^{(N=5)}_{1,0} = D^{(N=5)}_{0,-1} = 15\pi/128$, $D^{(N=5)}_{2,*} = D^{(N=5)}_{-2,*} = 65\pi/256$, $D^{(N=5)}_{1,*} = D^{(N=5)}_{-1,*} \simeq 0.3909$ and $D^{(N=5)}_{0,*} = 29/120$. Figures 5(*c*) and (*d*) present a schematic map of these states. Although the results are analytical, we give their numerical approximations, which give some flavour of the geometric structure induced by the Monge metric.

4.6. Monge distances for an arbitrary j

4.6.1. Eigenstates of $\boldsymbol{J}_z$. Using the formula for distribution functions $F(\vartheta)$ one may express the distances between neighbouring eigenstates of J_z for an arbitrary j by the following formula:

$$D_{\mathrm{M}}(|j, m\rangle, |j, m-1\rangle) = \pi \binom{2(N-n)}{N-n} \binom{2n}{n} 2^{-2N} \tag{4.14}$$

for $m = -j+1, \ldots, j$, where $N = 2j+1$ and $n = j+m = 1, \ldots, N-1$ (for the proof see appendix E.1). This leads to the following asymptotic formula:

$$D_{\mathrm{M}}(|j, m\rangle, |j, m-1\rangle) \sim \frac{1}{\sqrt{n(N-n)}} \tag{4.15}$$

valid for large j, where n is defined above. It is easy to show that that for each j all the eigenstates of J_z are located on one metric line. Hence we obtain

$$\begin{aligned} D_{\mathrm{M}}(\rho_+, \rho_-) = D_{\mathrm{M}}(|j, j\rangle, |j, -j\rangle) &= \sum_{m=-j+1}^{j} D_{\mathrm{M}}(|j, m\rangle, |j, m-1\rangle) \\ &= \pi \left[1 - \binom{2N}{N} 2^{1-2N} \right]. \end{aligned} \tag{4.16}$$

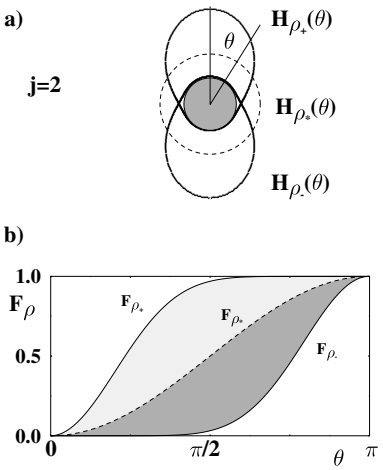

Figure 8. As figure 4 for $j = 2$.

4.6.2. Distance from ρ_*. According to property B the distance of each coherent state from ρ_* is the same and equal to $R_1 = D_{\mathrm{M}}(\rho_+, \rho_*)$. This quantity may be found explicitly for an arbitrary $N = 2j + 1$:

$$D_{\mathrm{M}}(\rho_+, \rho_*) = \frac{1}{2} D_{\mathrm{M}}(\rho_+, \rho_-) = \frac{\pi}{2}\left[1 - \binom{2N}{N} 2^{1-2N}\right] \tag{4.17}$$

which is asymptotically (for large N) equal to $\pi/2 - \sqrt{\pi/N}$. Such a quantity is shown in figure 8 (for $j = 2$) as the area between two corresponding distribution functions. Observe that in comparison with figure 4 the coherent states are more localized, and the area between steeper distribution functions is larger. In the classical limit $N \to \infty$ we arrive at $D_{\mathrm{M}}(\rho_+, \rho_*) \to \pi/2$ and $D_{\mathrm{M}}(\rho_+, \rho_-) \to \pi$. The latter result has a simple interpretation: in this limit the coherent states become infinitely sharp and the Monge plan consists in the rotation of the sphere (of radius 1) by the angle π. The three points ρ_+, ρ_* and ρ_- form another metric line, which for $N > 2$ is different from the metric line generated by the eigenstates of J_Z. Thus, for $N > 2$, the metric induced by the Monge distance is not 'flat'. Moreover, for $j \in \mathbb{N}$ we have

$$D_{\mathrm{M}}(|0\rangle\langle 0|, \rho_*) = \sum_{k=1}^{j} \frac{1}{2k+1} \frac{(2k-1)!!}{(2k)!!} \tag{4.18}$$

which tends to $\pi/2 - 1$ in the semiclassical limit $j \to \infty$ (for the proof see appendix E.2). It is well known that this convergence is very slow.

4.6.3. Coherent states. Now, let us consider two coherent states $|\vartheta, \varphi\rangle$ and $|\vartheta', \varphi'\rangle$. It follows from the rotational invariance of the Monge metric (property B) that their distance depends only on Ξ—the angle between two vectors on S^2 representing these coherent states—and is equal to the Monge distance between two coherent states lying on the Greenwich meridian $\rho_+ = |0, 0\rangle\langle 0, 0|$ and $\rho_\Xi := |\Xi, 0\rangle\langle \Xi, 0|$ (for $N = 2$ the latter corresponds to the state labelled in figure 3 by ρ_θ). We denote this distance by $C(\Xi, j) := D_{\mathrm{M}}(\rho_+, \rho_\Xi)$. Using propositions 6 we obtain the following formula for this quantity (for the proof see appendix E.3):

$$C(\Xi, j) = \pi \sin(\Xi/2)\, W_j\left(\sin^2\left(\Xi/2\right)\right) \tag{4.19}$$

where W_j is a polynomial of the form

$$W_j(x) := \frac{2j+1}{4^{j+1}} \sum_{\substack{0 \leqslant u,v \\ u+v<j}} S_{j,u,v}\, A_{u,v}\, x^u (1-x)^v . \tag{4.20}$$

The symmetric coefficients $S_{j,u,v}$ are given by

$$S_{j,u,v} := \frac{(2j)!}{(2j-2(u+v)-1)!u!v!(u+v+1)!4^{u+v}} \tag{4.21}$$

and the asymmetric coefficients $A_{u,v}$ by

$$A_{u,v} := \sum_{s=v+1}^{\infty} \frac{\binom{2s}{s}}{(u+1+s)\,4^s}. \tag{4.22}$$

Note that $A_{u,v}$ can be also written as a finite sum

$$A_{u,v} = \frac{2^{2u+1}}{\binom{2u}{u}(2u+1)} - \sum_{s=0}^{v} \frac{\binom{2s}{s}}{(u+1+s)\,4^s}. \tag{4.23}$$

The rank of W_j is $\lfloor j-1/2 \rfloor$, i.e. the largest integer less than or equal to $j-1/2$. We have $W_{1/2}(x) = \frac{1}{4}$ (and so $C(\Xi, 1/2) = (\pi/4)\sin(\Xi/2) \sim D_{\mathrm{HS}}(\rho_+, \rho_\Xi)$), $W_1(x) = \frac{3}{8}$, $W_{3/2}(x) = \frac{1}{128}(57+x)$, $W_2(x) = \frac{5}{256}(25+x)$ etc.

One can show that all the coefficients of the polynomial W_j are positive. This leads to the following simple lower and upper bounds:

$$\pi\, C_j\, \sin(\Xi/2) \leqslant C(\Xi, j) \leqslant \pi\, D_j\, \sin(\Xi/2) \tag{4.24}$$

where

$$C_j := W_j(0) = \frac{j(2j+1)}{2^{2j+1}}\, {}_3\mathcal{F}_2([3/2, 1/2-j, 1-j], [2,2], 1) \tag{4.25}$$

and

$$D_j := W_j(1) = \frac{j(2j+1)}{2^{2j+1}}\,(2\cdot\, {}_3\mathcal{F}_2([1, 1/2-j, 1-j], [2, 3/2], 1) - {}_3\mathcal{F}_2([1, 1/2-j, 1-j], [2,2], 1)) \tag{4.26}$$

(here ${}_3\mathcal{F}_2$ stands for the generalized hypergeometric function). Note that $C_j \to 2/\pi$ and $D_j \to 1$ in the semiclassical limit $j \to \infty$. For two infinitesimally close coherent states the angle $\Xi \sim 0$ and we obtain

$$C(\Xi, j) \sim \frac{\pi}{2}\, C_j\, \Xi \tag{4.27}$$

with

$$C(\Xi, j) \to \Xi \quad (j \to \infty) \tag{4.28}$$

which agrees with property (3.13).

4.6.4. Chaotic states. In the stellar representation the coherent states are represented by $N-1$ zeros merging together at the antipodal point on the sphere. These quantum states are rather exceptional; a typical state has all zeros distributed all over the sphere. It is known [59] that for the so-called *chaotic states* (eigenstates of Floquet operator corresponding to classically chaotic systems) the distribution of zeros is almost uniform in the phase space. Such states are entirely delocalized and their Husimi distribution is close, in a sense of the L_1 metric, to the uniform Husimi distribution H_{ρ_*} corresponding to the maximally mixed state ρ_*. One can therefore expect (applying proposition 2) that the Monge distance between these chaotic pure states ρ_c and ρ_* is small. We conjecture that the mean value of the Monge distance $D_{\mathrm{M}}(\rho_c, \rho_*)$ of randomly picked chaotic pure state ρ_c from ρ_* tends to zero in the semiclassical limit $j \to \infty$.

4.7. Correspondence to the Wehrl entropy and the Lieb conjecture

In order to describe the phase space structure of any quantum state ρ it is useful [60] to define the Wehrl entropy S_ρ as the Boltzmann–Gibbs entropy of the Husimi distribution (4.6)

$$S_\rho = -\int_{S^2} H_\rho(\theta,\varphi)\ln[H_\rho(\theta,\varphi)]\,\mathrm{d}\mu\,(\vartheta,\varphi). \tag{4.29}$$

It was conjectured by Lieb [61] that this quantity is minimal for coherent states, which are as localized on the sphere as allowed by the Heisenberg uncertainty relation. For partial results in the direction to prove this conjecture see [62–65]. The minimum of entropy reads $S_{\min} = (N-1)/N - \ln N$, where the logarithmic term is due to the normalization of the Husimi distribution. It was also conjectured [63] that the states with possibly regular distribution of zeros on the sphere, which is easy to specify for Pythagorean numbers $N = 2, 4, 6, 8, 12, 20$, are characterized by the largest possible Wehrl entropy among all pure states.

Let us emphasize that for $N \gg 1$ the states exhibiting small Wehrl entropy comparable to $S_{\min}$ are not typical. In the stellar representation coherent states correspond to the coalescence of all $N-1$ zeros of the Husimi distribution at one point. In a typical situation all zeros are distributed uniformly on the sphere, and the Wehrl entropy of such delocalized pure states is large. Averaging over the natural Haar measure on the space of pure states $\mathcal{P}$ one may compute the mean Wehrl entropy $\langle S\rangle$ for the N-dimensional states. In a slightly different context such integration was performed in [66–68], leading to

$$\langle S\rangle_{U(N)} = -\ln N + \Psi\,(N+1) - \Psi\,(2) \tag{4.30}$$

where Ψ denotes the digamma function, which for natural arguments $k < n$ satisfies $\Psi(n) - \Psi(k) = \sum_{m=k}^{n-1} 1/m$. In the classical limit $N \to \infty$ the mean entropy tends to $\gamma - 1 \sim -0.422\,78$ (γ is the Euler constant), which is close to the maximal possible Wehrl entropy $S_{\rho_*} = 0$.

The Wehrl entropy does not induce a metric in the space of quantum states. However, it describes the localization of a quantum state in the classical phase space and has some properties similar to the Monge distance of a given state ρ to the maximally mixed state ρ_* [69]. In view of our results on the Monge distance, we advance analogous conjectures, concerning the set of pure states $\mathcal{P}$ belonging to the N-dimensional Hilbert space.

Conjecture 1. *In the sense of the Monge metric the coherent states are pure states most distant from ρ_*. This maximal distance R_1 is given by (4.17) and tends to $\pi/2$ for $N \to \infty$.*

Conjecture 2. *Pure states which maximize the Wehrl entropy are the closest to ρ_* in the sense of the Monge metric. This minimal distance R_2 is equal to one-sixth for $N = 3$ and tends to zero for $N \to \infty$.*

In analogy to the properties of the Wehrl entropy and formula (4.30), one can expect that the mean distance $\langle R\rangle = \langle D_{\mathrm{M}}(|\psi\rangle\langle\psi|, \rho_*)\rangle$ averaged over the natural measure on the manifold of pure states $\mathcal{P}$ is close to the minimal distance R_2 and, for large N, is much smaller than the maximal distance R_1. In other words, the coherent states, distinguished by the fact of being situated in $\mathcal{M}$ as far from ρ_* as possible, are not generic. This observation is not surprising, since $\mathcal{C} \sim \mathbb{C}P^1$ while $\mathcal{P} \sim \mathbb{C}P^{N-1}$, but is not captured using any standard metrics in the space $\mathcal{M}$ of mixed quantum states.

5. Comparison of Monge and standard distances

Results obtained for distances between several pairs of mixed states are summarized in table 2. Calculations of the trace, Hilbert–Schmidt and Bures distances are performed directly from the definitions provided in section 1.

Note that the geometry of the space $\mathcal{M}$ is well understood for $N = 2$. In the sense of the trace and the Hilbert–Schmidt metrics the set of all mixed states has then the property of a ball contained inside the Bloch sphere: the states ρ_+, ρ_* and ρ_- form a metric line. The same statement is true for the Monge metric (see formula 4.11). However, for the Bures metric the situation is different. As shown by Hübner the set $\mathcal{M}$ has in this case the structure of half of a three-sphere [9], so ρ_+, ρ_* and ρ_- form an isosceles triangle. However, the state ρ_*, located at the pole of S^3, is equally distant (with respect to the Bures metric) from all the pure states $\mathcal{P}$, which occupy the 'hyper-equator' $\sim S^2$.

5.1. Geometry of quantum states for large N

The data collected in table 2 allow us to emphasize important differences between the geometry induced by the standard distances and the Monge distance. From the points of view of all three of the standard metrics, the distance R between ρ_* and any pure state is constant. Therefore, in these standard geometries, the coherent states are not distinguished in any sense in $\mathcal{P}$.

On the other hand, a 'semiclassical' geometry, induced by the Monge metric in the $(N^2 - 1)$-dimensional space $\mathcal{M}$, distinguishes the space of coherent states $\mathcal{C} \sim S^2$. Their Monge distance (R_1) from the centre ρ_* is maximal. If we try to visualize the $(2N - 2)$-dimensional space of pure states $\mathcal{P} \sim \mathbb{C}P^{N-1}$ as a 'hyper-ellipsoid', the coherent states form the 'largest circle', represented by the dashed ellipse in figure 9. There exists also a multi-dimensional subspace of $\mathcal{P}$, consisting of delocalized pure states ρ_c, with zeros of the corresponding Husimi function distributed uniformly on the sphere. Such states are situated close to ρ_* with respect to the Monge metric. In the classical limit $N \to \infty$, their distance from ρ_* (R_2) is arbitrary small, so the manifold $\mathcal{P}$, almost touches the maximally mixed state ρ_*. In this case, we might think of $\mathcal{M}$ as of a full $(N^2 - 1)$-dimensional disc of radius $R_1 \sim \pi/2$ centred at ρ_*, with coherent states at its edge and the pure states on its surface. Since it is rather flat, and contains a lot of its 'mass' close to its centre, it resembles, in a sense, the Galaxy.

5.2. Dynamical properties

As mentioned in section 2 the standard distances are preserved by the unitary dynamics (see formula (2.11)). An analogous relation is true for the Monge distance only for some special cases, for example for simple rotations $U = \exp(\mathrm{i}aJ_z)$ which preserve the coherence. In general, however, the Monge distance is not conserved:

$$D_{\mathrm{M}}(\rho_1, \rho_2) \neq D_{\mathrm{M}}(\rho_1', \rho_2'). \tag{5.1}$$

Vaguely speaking, during the rotation of the 'hyper-ellipsoid', depicted in figure 9, a kind of contraction occurs, so the Monge distance changes during the unitary time evolution (and hence is not a monotonic metric). Since in the classical limit the distance between coherent states tends to the classical distance on the sphere, we suggested [21] studying the time evolution of the Monge distance $D_{\mathrm{M}}(t)$ between two neighbouring coherent states. The quantity $\lambda(t) = \lim_{D_{\mathrm{M}}(0)\to 0}(\ln[D_{\mathrm{M}}(t)/D_{\mathrm{M}}(0)])/t$ indeed characterizes the stability of the quantum system. To obtain a closer analogy with the classical Lyapunov exponent one should then perform the limit $t \to \infty$. However, for longer times, both vector coherent states become delocalized (under the assumption of a generic evolution operator U), and their distance from ρ_* becomes small. Therefore, after some time t_r, the distance $D_{\mathrm{M}}(t)$ starts to decrease, so instead of analysing $\lim_{t\to\infty}\lambda(t)$ (which always tends to zero), one needs to relay on quantity $\lambda(tv)$ defined for a finite time tv [21, 70].

Table 2. Standard distances (trace, Hilbert–Schmidt and Bures) versus the Monge distance for various quantum states in $N = 2j + 1$ dimensions: pure states, the coherent states $\rho_\Xi = |\Xi\rangle\langle\Xi|$, ρ_+, ρ_- and the eigenstates $|m\rangle$ of J_z; mixed states, ρ_a, defined in section 4.2, and the maximally mixed state ρ_*. For the Monge distance we give semiclassical asymptotics ($N \to \infty$). The polynomials $W_j(x)$ are given by formula (4.20).

States		D_{tr}	D_{HS}	D_{Bures}	D_{Monge}
(ρ_+, ρ_-)		2	$\sqrt{2}$	$\sqrt{2}$	$\pi(1 - \binom{2N}{N}2^{1-2N}) \sim \pi - 2\sqrt{\pi/N}$
$(\rho_+, \rho_*) = (\rho_-, \rho_*)$		$2 - \frac{2}{N}$	$\sqrt{1 - \frac{1}{N}}$	$\sqrt{2 - \frac{2}{\sqrt{N}}}$	$\pi(1/2 - \binom{2N}{N}2^{-2N}) \sim \pi/2 - \sqrt{\pi/N}$
ρ_+, ρ_*, ρ_-	$N = 2$	line	line	isosceles Δ	line
	$N > 2$	isosceles Δ	isosceles Δ	isosceles Δ	line
	$N \to \infty$	equilateral Δ	isosceles Δ	equilateral $\triangle$	line
$(\|0\rangle, \rho_*)$ $(j \in \mathbb{N})$		$2 - \frac{2}{2j+1}$	$\sqrt{1 - \frac{1}{2j+1}}$	$\sqrt{2 - \frac{2}{\sqrt{2j+1}}}$	$\sum_{k=1}^{j} \frac{1}{2k+1} \frac{1}{(2k-1)!!(2k)!!} \to \pi/2 - 1$
$\|m\rangle, \|m-1\rangle$		2	$\sqrt{2}$	$\sqrt{2}$ $(n = j + m)$	$\pi\binom{2(N-n)}{N-n}\binom{2n}{n}2^{-2N} \sim \frac{1}{\sqrt{N-n}\sqrt{n}}$
$\|-j\rangle \cdots \|m\rangle \cdots \|j\rangle$		N-dim simplex	N-dim simplex	N-dim simplex	line
(ρ_+, ρ_a)		$2(1-a)$	$\sqrt{2}(1-a)$	$\sqrt{2(1-\sqrt{a})}$	$2\pi(1 - \binom{2N}{N}2^{1-2N})(1-a)$
(ρ_-, ρ_a)		$2a$	$\sqrt{2}a$	$\sqrt{2(1-\sqrt{1-a})}$	$2\pi(1 - \binom{2N}{N}2^{1-2N})a$
ρ_+, ρ_a, ρ_-		line	line	$\triangle$	line
(ρ_+, ρ_Ξ)	$N = 2$	$2\sin(\Xi/2)$	$\sqrt{2}\sin(\Xi/2)$	$\sqrt{2 - 2\cos(\Xi/2)}$	$(\pi/4)\sin(\Xi/2)$
	$N \geqslant 2$	$2\sqrt{1 - \cos^{4j}(\Xi/2)}$	$\sqrt{2 - 2\cos^{4j}(\Xi/2)}$	$\sqrt{2 - 2\cos^{2j}(\Xi/2)}$	$C(\Xi, j) = \pi \sin(\Xi/2)\, W_j\left(\sin^2(\Xi/2)\right)$ $\to \Xi$ for $N \to \infty$
(ρ_-, ρ_Ξ)	$N = 2$	$2\cos(\Xi/2)$	$\sqrt{2}\cos(\Xi/2)$	$\sqrt{2 - 2\sin(\Xi/2)}$	$(\pi/4)\cos(\Xi/2)$
	$N \geqslant 2$	$2\sqrt{1 - \sin^{4j}(\Xi/2)}$	$\sqrt{2 - 2\sin^{4j}(\Xi/2)}$	$\sqrt{2 - 2\sin^{2j}(\Xi/2)}$	$C(\Xi, j) = \pi \cos(\Xi/2)\, W_j\left(\cos^2(\Xi/2)\right)$ $\to \pi - \Xi$ for $N \to \infty$

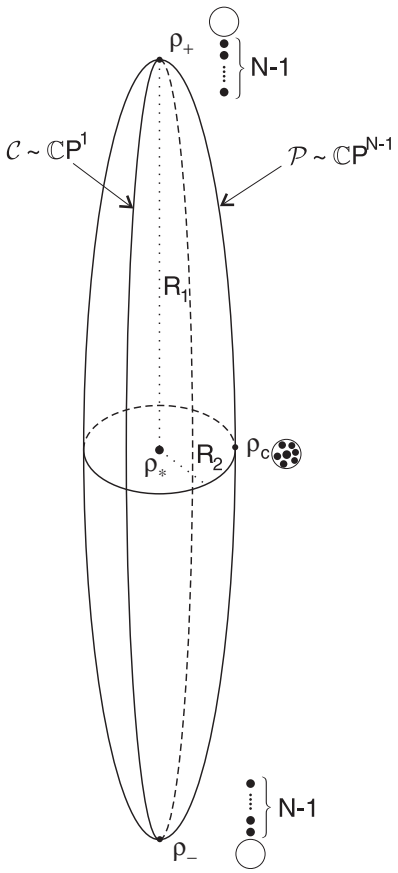

Figure 9. Sketch of the space $\mathcal{M}$ in the semiclassical regime $j \gg 1$. In the limit $j \to \infty$ the larger radius R_1 tends to $\pi/2$, while the smaller $R_2 \to 0$. Dots and small circles show the corresponding pure states in the stellar representation.

5.3. Delocalization and decoherence

As mentioned above, the localization of a given pure state $|\phi\rangle$ in the classical phase space is reflected by its large Monge distance from ρ_*. In an analogous way one may characterize the properties of a given Hamiltonian H or a unitary Floquet operator F by the mean distance of its eigenstates $|v_i\rangle$, $i = 1, \ldots, N$, from the maximally mixed state. Such a quantity, $\gamma := \sum_{i=1}^{N} D_{\mathrm{M}}(|v_i\rangle\langle v_i|, \rho_*)]/N$, indicates the average localization of the eigenstates, relevant to distinguish between integrable and chaotic quantum dynamics [71]. It might be thus interesting to find unitary operators $F_{\min}$ and $F_{\max}$, for which the mean distance γ achieves the smallest (the largest) value.

Physical systems coupled to the environment suffer decoherence. The density matrix of a given system tends to be diagonal in the eigenbasis of the Hamiltonian H_I, which describes the interaction with the environment [72]. In the simplest case, $N = 2$, the decoherence may be visualized as an orthogonal projection into an axis determined by H_I. For example, if H_I is proportional to J_z, it is just the z axis, which joints both poles of the Bloch sphere.

In the general case of arbitrary N, there exists an $(N-1)$-dimensional simplex $\mathcal{I}$ of density matrices diagonal in the eigenbasis of H_I. Decoherence consists thus in projecting of the initial state into $\mathcal{I}$. In a generic case of a typical interaction the eigenstates of H_I are delocalized and their Monge distance from ρ_* is small. On the other hand, the typical coherent states are located far away from $\mathcal{I}$, in the sense of the Monge metric. One can therefore expect that

the Monge distance of a given quantum state from $\mathcal{I}$ contains the information concerning the speed of decoherence. It is known that among all pure states the decoherence of the coherent states is the slowest [73].

Moreover, the speed of decoherence of a Schrödinger-cat-like pure state, localized at two different classical points x and x', in a generic case depends on their separation in the classical phase space. Consider now a coherent superposition $|\psi\rangle = (|\alpha\rangle + |\beta\rangle)/\sqrt{2}$ of two arbitrary quantum pure states. The Monge distance between them, $D_{\mathrm{M}}(|\alpha\rangle, |\beta\rangle)$, might be thus used to characterize the speed of the decoherence of the cat-like state $|\psi\rangle$.

6. Simplified Monge distance between pure states

6.1. Definition

With help of the stellar representation [53, 55, 56] we may link any pure state $|\varphi\rangle$ of the N-dimensional Hilbert space to a singular distribution $f_\varphi(x)$ containing $(N-1)$ delta peaks placed in the zeros x_i of the corresponding Husimi function $H_{|\varphi\rangle\langle\varphi|}(x)$, where $x \in S^2$,

$$|\varphi\rangle \to f_\varphi(x) := \frac{1}{N-1} \sum_{i=1}^{N-1} \delta(x - x_i). \tag{6.1}$$

The zeros x_i may be degenerate. For any coherent state all $(N-1)$ zeros cluster at the antipodal point, so $|\alpha\rangle$ is represented by $f_\alpha(x) = \delta(x - \bar{\alpha})$.

The *simplified Monge distance* between any pure states $|\varphi\rangle$ and $|\psi\rangle$ is defined as the Monge distance (3.3) between the corresponding distributions (6.1)

$$D_{\mathrm{sM}}(|\varphi\rangle, |\psi\rangle) := D_{\mathrm{M}}(f_\varphi, f_\psi). \tag{6.2}$$

It may be also called the *discrete Monge distance*, since it corresponds to a discrete Monge problem, which may be effectively evaluated numerically by means of the algorithms of linear programming [45]. This contrasts the original definition (3.11), for which one needs to solve the two-dimensional Monge problem for *continuous* Husimi distributions.

Clearly, in the space of pure quantum states the two Monge distances are related. This fact becomes more transparent if one realizes that (6.2) is equal to the Monge distance between the related distributions $\bar{f}_\varphi := \big[\sum_{i=1}^{N-1} \delta_{\bar{x}_i}\big]/(N-1)$ and $\bar{f}_\psi := \big[\sum_{i=1}^{N-1} \delta_{\bar{y}_i}\big]/(N-1)$, where $y_1, \ldots, y_{N-1}$ are zeros of the Husimi distribution $H_{|\psi\rangle\langle\psi|}$, and points x_i and $\bar{x}_i$ (y_i and $\bar{y}_i$) are antipodal on the sphere (note that the bar does not denote here the complex conjugation). The distributions $\bar{f}_\varphi$ and $\bar{f}_\psi$ may be considered as a discrete, $(N-1)$-point approximation of the continuous Husimi distributions $H_{|\varphi\rangle\langle\varphi|}$ and $H_{|\psi\rangle\langle\psi|}$.

Since any coherent state is represented by a single Dirac delta, $\bar{f}_\alpha(x) = \delta(x - \alpha)$, the semiclassical condition (1.8) is exact for any dimension N

$$D_{\mathrm{sM}}(|\eta_1\rangle, |\eta_2\rangle) = d(\eta_1, \eta_2). \tag{6.3}$$

Thus for $N = 2$ the discrete Monge distance, D_{sM}, is twice the Fubini–Study distance (1.7) (in this case, the Riemannian distance d on the sphere of radius 1/2), while the continuous Monge metric, D_{M}, is proportional to the Hilbert–Schmidt distance (1.2) (in this case, the Euclidean distance along the cord inside the sphere). At small distances both geometries coincide (the 'flat earth' approximation).

6.2. Eigenstates of $\boldsymbol{J}_z$

In stellar representation the state $|j, m\rangle$ is described by $j+m$ zeros at the south pole and $j-m$ zeros at the north pole. Thus the distribution $f_{j,m}(x)$ consists of two delta peaks, π apart, and

it is straightforward to obtain the following general result:

$$D_{\mathrm{sM}}(|j,m\rangle, |j,m'\rangle) = \frac{\pi}{2j}|m-m'|. \tag{6.4}$$

In particular $D_{\mathrm{sM}}(|j,j\rangle, |j,-j\rangle) = \pi = d(\alpha,\bar{\alpha})$. The zeros of the Husimi function of the eigenstates of the operators J_y and J_x are located at the equator at distance $\pi/2$ from both poles. Thus

$$D_{\mathrm{sM}}(|j,m\rangle_z, |j,m'\rangle_y) = D_{\mathrm{sM}}(|j,m\rangle_z, |j,m''\rangle_x) = \frac{\pi}{2} \tag{6.5}$$

for any choice of quantum numbers m, m' and m''.

6.3. Random chaotic states

Eigenstates of classically chaotic dynamical systems may be described by random pure states [71]. Expansion coefficients of a chaotic state $|\psi_{\mathrm{c}}\rangle$ in an arbitrary basis may be given by a vector of a random unitary matrix, distributed according to the Haar measure on $U(N)$. Zeros of the corresponding Husimi representation are distributed uniformly on the entire sphere [56] (with the correlations between them given by Hannay [74]). This fact allows one to compute the average distance of a random state from any coherent state

$$D_{\mathrm{sM}}(|\alpha\rangle, |\psi_{\mathrm{c}}\rangle) = \frac{1}{2}\int_0^{\pi} \Xi \sin\Xi \,\mathrm{d}\Xi = \frac{\pi}{2}. \tag{6.6}$$

In a similar way we obtain the average distance to the eigenstates of J_z

$$\left\langle D_{\mathrm{sM}}(|j,m\rangle, |\psi_{\mathrm{c}}\rangle)\right\rangle = \chi \sin\chi + \cos\chi \qquad \text{where} \quad \chi = \frac{m\pi}{2j}. \tag{6.7}$$

This admits the smallest value equal to unity for $m = \chi = 0$, while the largest value is obtained for $m = \pm j$, for which the above formula reduces to (6.6).

Let us divide the sphere into N cells of diameter proportional to $\sqrt{N}$. Consider two different uncorrelated random states $|\psi_c\rangle$ and $|\phi_c\rangle$. Uniform distribution of zeros implies that there will be on average one zero in each cell and the distance between the corresponding zeros of both states is of order of $\sqrt{N}$. Thus their simplified Monge distance vanishes in the semiclassical limit,

$$D_{\mathrm{sM}}(|\psi_{\mathrm{c}}\rangle, |\phi_c\rangle) \approx \frac{1}{N}\frac{N}{\sqrt{N}} \sim N^{-1/2} \to 0 \qquad (N \to \infty). \tag{6.8}$$

Thus in the space of pure quantum states the simplified, discrete Monge metric D_{sM} displays several features of the original, continuous Monge metric D_{M}.

7. Concluding remarks

In this paper we analysed the properties of the set of all mixed states constructed of the pure states belonging to the N-dimensional Hilbert space. The structure of this set is highly non-trivial due to the existence of the density matrices with degenerate spectra. Each spectrum may be represented by a point in the $(N-1)$-dimensional simplex. In a generic case of a nondegenerate spectrum (a point located in the interior of the simplex) this set has a structure of $[U(N)/(U(1))^N] \times G_N$. However, there exist altogether 2^{N-1} parts of the asymmetric simplex of eigenvalues, all but one corresponding to its boundaries. These boundary points, representing various kinds of degeneration of the spectrum, lead to a different local structure of the set of mixed states.

Standard metrics in the space of quantum states are not related to the metric structure of the corresponding classical phase space. To establish such a link we used vector coherent states, localized in a given region of the sphere, which play a role of the classical phase space. Each quantum state may be then uniquely represented by its Husimi distribution, which carries the information concerning its localization in the classical phase space. We proposed to measure the distance between two arbitrary quantum states by the Monge distance between the corresponding Husimi distributions. Therefore, to compute this distance, one has to solve the Monge problem on the sphere. Thus, unexpectedly, a motivation stemming from quantum mechanics leads us close to the original Monge problem of transporting soil on the Earth surface. Even if the exact solution of the Monge problem is not accessible we can use either lower or upper bounds for the Monge distance (definition (3.2), propositions 2 and 4), or numerical algorithms based on the idea of approximation of continuous distributions by discrete ones. These techniques lead to general methods of computing the Monge distance on the sphere (propositions 5 and 6), as well as to concrete results we have obtained in this paper (sections 4.3–4.6 and section 5.1).

The Monge distance induces a non-trivial geometry in the space of mixed quantum states. For $N = 2$ it is consistent with the geometry of the Bloch ball induced by the Hilbert–Schmidt or the trace distance. For larger N it distinguishes the coherent states, which are as localized in the phase space, as allowed by the Heisenberg uncertainty principle. These states, lying far away from the most mixed state ρ_*, are not typical. The vast majority of pure quantum states are localized in the vicinity of ρ_* in the sense of the Monge metric. The Hilbert–Schmidt distance between a given state ρ and ρ_* may be used to measure its degree of mixing. On the other hand, the Monge distance $D_{\mathrm{M}}(\rho, \rho_*)$ provides information concerning the localization of the state ρ in the classical phase space.

A similar geometry in the space of pure quantum states is induced by the simplified Monge metric d_{sM}. It is defined by the Monge distance between the $(N-1)$-point discrete approximations to the Husimi representation generated by the stellar representation of pure states. This version of the Monge distance may be easily evaluated numerically by means of linear programming algorithms [45]. Therefore it might be used to study the divergence of initially closed pure states subjected to unitary dynamics and to define a quantum analogue of the classical Lyapunov exponent [21, 44]. Moreover, this metric may be useful in an attempt to prove the Lieb conjecture: it suffices to show that for any pure state $|\psi\rangle$ the Wehrl entropy decreases along the line joining $|\psi\rangle$ to the closest coherent state.

In contrast with the standard distances, neither Monge distance is invariant under an arbitrary unitary transformation. This resembles the classical situation, where two points in the phase space may drift away under the action of a given Hamiltonian system. In a sense, the Monge distance in the space of quantum states enjoys some classical properties. Several classical quantities emerge in the description of quantum systems. We believe, accordingly, that the concept of the Monge distance between quantum states might be useful to elucidate various aspects of the quantum–classical correspondence.

Acknowledgments

KŻ would like to thank I Bengtsson for fruitful discussions and hospitality in Stockholm. It is a pleasure to thank H Wiedemann for a collaboration at the early stage of this project and S Cynk, P Garbaczewski, Z Pogoda and P Slater for helpful comments. A travel grant from the European Science Foundation under the programme 'Quantum information' (KŻ) and financial support by Polish KBN grant no 2 P03B 07219 are gratefully acknowledged.

Appendix A. Proof of proposition 2

Applying proposition 1 we see that it suffices to prove the inequality

$$\left| \int_\Omega f(x)(Q_1(x) - Q_2(x)) \, \mathrm{d}m\,(x) \right| \leqslant \frac{\Delta}{2} D_{L_1}(Q_1, Q_2) \tag{A.1}$$

for every weak contraction $f : \Omega \to \mathbb{R}$. For such f we see at once that $(\max f - \min f) \leqslant \Delta$. Let us consider a function $g : \Omega \to \mathbb{R}$ defined by the formula $g(x) = f(x) - \min f - \Delta/2$ for $x \in \Omega$. Clearly $|g| \leqslant \Delta/2$. Finally, we obtain

$$\begin{aligned} &\left| \int_\Omega f(x)(Q_1(x) - Q_2(x)) \, \mathrm{d}m\,(x) \right| \\ &\qquad = \left| \int_\Omega g(x)(Q_1(x) - Q_2(x)) \, \mathrm{d}m\,(x) \right| \leqslant \frac{\Delta}{2} D_{L_1}(Q_1, Q_2) \end{aligned} \tag{A.2}$$

which completes the proof.

Appendix B. Proof of proposition 4

Let $\rho_1, \rho_2 \in \mathcal{M}$. We denote the set of all contractions (c-Lipschitzian functions with $c \leqslant 1$) $f : \Omega \to \mathbb{R}$ by Lip_1. We have

$$\begin{aligned} D_{\mathrm{M}}(\rho_1, \rho_2) &= D_{\mathrm{M}}\left(H_{\rho_1}, H_{\rho_2}\right) \\ &= \max_{f \in \mathrm{Lip}_1} \left| \int_\Omega f(\eta)(H_{\rho_1}(\eta) - H_{\rho_2}(\eta)) \, \mathrm{d}m\,(\eta) \right| \\ &= \max_{f \in \mathrm{Lip}_1} \left| \int_\Omega f(\eta) \langle \eta | (\rho_1 - \rho_2) | \eta \rangle \, \mathrm{d}m\,(\eta) \right| \\ &= \max_{f \in \mathrm{Lip}_1} \left| \mathrm{tr} \left(\int_\Omega f(\eta) |\eta\rangle\langle\eta| \, \mathrm{d}m\,(\eta) \, (\rho_1 - \rho_2) \right) \right| \\ &= \max \Big\{ |\,\mathrm{tr}\, A(\rho_1 - \rho_2)| : A - \text{Hermitian} \\ &\qquad \text{and } A = \int_\Omega f(\eta) |\eta\rangle\langle\eta| \, \mathrm{d}m\,(\eta) \text{ for some } f \in \mathrm{Lip}_1 \Big\} \\ &= \max_{L(A) \leqslant 1} |\,\mathrm{tr}\, A(\rho_1 - \rho_2)|. \end{aligned} \tag{B.1}$$

Appendix C. Proof of proposition 5

We start from two simple lemmas on weak contractions on the sphere. In the following, d denotes the Riemannian metric on S^2.

Lemma A.1. *Let $f : [0, \pi] \to \mathbb{R}$ be a weak contraction. Define $\tilde{f} : S^2 \to \mathbb{R}$ by the formula*

$$\tilde{f}(\vartheta, \varphi) = f(\vartheta) \tag{C.1}$$

for $(\vartheta, \varphi) \in S^2$. Then $\tilde{f}$ is a weak contraction.

Proof of lemma A.1. Let $(\vartheta_1, \varphi_1), (\vartheta_2, \varphi_2) \in S^2$. Applying the spherical triangle inequality we obtain $|\tilde{f}(\vartheta_1, \varphi_1) - \tilde{f}(\vartheta_2, \varphi_2)| = |f(\vartheta_1) - f(\vartheta_2)| \leqslant |\vartheta_1 - \vartheta_2| \leqslant d((\vartheta_1, \varphi_1), (\vartheta_2, \varphi_2))$.□

Lemma A.2. *Let $G : S^2 \to \mathbb{R}$ be a weak contraction. Define $\tilde{G} : [0, \pi] \to \mathbb{R}$ by the formula*

$$\tilde{G}(\vartheta) = \frac{1}{2\pi} \int_0^{2\pi} G(\vartheta, \varphi)\, \mathrm{d}\varphi \tag{C.2}$$

for $\vartheta \in [0, \pi]$. Then $\tilde{G}$ is a weak contraction.

Proof of lemma A.2. Let $\vartheta_1, \vartheta_2 \in [0, \pi]$. We have $d((\vartheta_1, \varphi), (\vartheta_2, \varphi)) = |\vartheta_1 - \vartheta_2|$. Hence $|\tilde{G}(\vartheta_1) - \tilde{G}(\vartheta_2)| = (1/2\pi) |\int_0^{2\pi} [G(\vartheta_1, \varphi) - G(\vartheta_2, \varphi)]\, \mathrm{d}\varphi| \leqslant (1/2\pi) \int_0^{2\pi} d((\vartheta_1, \varphi), (\vartheta_2, \varphi))\, \mathrm{d}\varphi \leqslant |\vartheta_1 - \vartheta_2|$. □

Proof of formula (4.7). It follows from proposition 1 that

$$\begin{aligned} D_{\mathrm{M}}(\rho_1, \rho_2) &= D_{\mathrm{M}}\big(H_{\rho_1}, H_{\rho_2}\big) \\ &= \max_{f \in \mathrm{Lip}_1(S^2)} \left| \int_0^{\pi} \int_0^{2\pi} f(\vartheta, \varphi)[H_{\rho_1}(\vartheta, \varphi) - H_{\rho_2}(\vartheta, \varphi)]\, \mathrm{d}m(\vartheta, \varphi) \right| \\ &= \max_{f \in \mathrm{Lip}_1(S^2)} \left| \int_0^{\pi} \left(\int_0^{2\pi} f(\vartheta, \varphi)[\tilde{H}_{\rho_1}(\vartheta) - \tilde{H}_{\rho_2}(\vartheta)] \sin\vartheta / 4\pi\, \mathrm{d}\vartheta \right) \mathrm{d}\varphi \right|. \end{aligned} \tag{C.3}$$

From the Salvemini formula (3.4), proposition 1, the above lemma A.1 and formula (C.3) we deduce that

$$\begin{aligned} &\int_0^{\pi} \big| F_{\rho_1}(\vartheta) - F_{\rho_2}(\vartheta) \big|\, \mathrm{d}\vartheta \\ &\quad = \max_{f \in \mathrm{Lip}_1([0,\pi])} \left| \int_0^{\pi} f(\vartheta) \big((h_{\rho_1}(\vartheta)) - h_{\rho_2}(\vartheta) \big)\, \mathrm{d}\vartheta \right| \\ &\quad = \max_{f \in \mathrm{Lip}_1([0,\pi])} \left| \int_0^{\pi} \left(\frac{1}{4\pi} \int_0^{2\pi} \tilde{f}(\vartheta, \varphi)[\tilde{H}_{\rho_1}(\vartheta) - \tilde{H}_{\rho_2}(\vartheta)] \sin\vartheta\, \mathrm{d}\vartheta \right) \mathrm{d}\varphi \right| \\ &\quad \leqslant \max_{f \in \mathrm{Lip}_1(S^2)} \left| \int_0^{\pi} \left(\frac{1}{4\pi} \int_0^{2\pi} f(\vartheta, \varphi)[\tilde{H}_{\rho_1}(\vartheta) - \tilde{H}_{\rho_2}(\vartheta)] \sin\vartheta\, \mathrm{d}\vartheta \right) \mathrm{d}\varphi \right| \\ &\quad = D_{\mathrm{M}}(\rho_1, \rho_2). \end{aligned} \tag{C.4}$$

On the other hand, applying formula (C.3), the above lemma A.2, proposition 1 and the Salvemini formula (3.4) we obtain

$$\begin{aligned} &D_{\mathrm{M}}(\rho_1, \rho_2) \\ &\quad = \max_{G \in \mathrm{Lip}_1(S^2)} \left| \int_0^{\pi} \left(\int_0^{2\pi} G(\vartheta, \varphi)[\tilde{H}_{\rho_1}(\vartheta) - \tilde{H}_{\rho_2}(\vartheta)] \sin\vartheta / 4\pi\, \mathrm{d}\vartheta \right) \mathrm{d}\varphi \right| \\ &\quad = \max_{G \in \mathrm{Lip}_1(S^2)} \left| \int_0^{\pi} \tilde{G}(\vartheta)[(H_1(\vartheta) - [H_2(\vartheta)] \sin\vartheta\, \mathrm{d}\vartheta \right| \\ &\quad \leqslant \max_{g \in \mathrm{Lip}_1([0,\pi])} \left| \int_0^{\pi} g(\vartheta)[H_1(\vartheta) \sin\vartheta - H_2(\vartheta) \sin\vartheta] \mathrm{d}\vartheta \right| \\ &\quad = \int_0^{\pi} |F_1(\vartheta) - F_2(\vartheta)|\, \mathrm{d}\vartheta \end{aligned} \tag{C.5}$$

which establishes the formula.

Appendix D. Proof of proposition 6

Put

$$\tilde{D}_{\mathrm{M}}(\rho_1, \rho_2) := \frac{1}{2\pi} \int_0^{2\pi} \int_0^{\pi} \big(F_1(t, \vartheta) - F_2(t, \vartheta)\big)\, \mathrm{d}t\, \mathrm{d}\vartheta. \tag{D.1}$$

Let $\varphi \in [0, 2\pi]$ and $i = 1, 2$. Integrating by parts we obtain

$$\int (-t)\, \tfrac{1}{2} H_{\rho_i}(t, \varphi) \sin t\, \mathrm{d}t = -t F_i(t, \varphi) + \int F_i(t, \varphi)\, \mathrm{d}t. \tag{D.2}$$

Hence

$$\begin{aligned}\int_0^{\pi} \big(F_1(t, \varphi) - F_2(t, \varphi)\big)\, \mathrm{d}t = \int_0^{\pi} (-t)\, \tfrac{1}{2} \big(H_{\rho_1}(t, \varphi) - H_{\rho_2}(t, \varphi)\big) \sin t\, \mathrm{d}t \\ + t\, (F_1(t, \varphi) - F_2(t, \varphi))\big|_{t=0}^{t=\pi}.\end{aligned} \tag{D.3}$$

According to assumption (1) the last term is equal to zero. Thus, applying proposition 1 to $f : S^2 \to \mathbb{R}$ given by $f(t, \varphi) = -t$, for $t \in [0, \pi]$, $\varphi \in [0, 2\pi]$, we obtain

$$\tilde{D}_{\mathrm{M}}(\rho_1, \rho_2) = \int_0^{2\pi} \int_0^{\pi} (-t)\, \tfrac{1}{2} \big(H_{\rho_1}(t, \varphi) - H_{\rho_2}(t, \varphi)\big) \sin t\, \mathrm{d}t\, \mathrm{d}\varphi \leqslant D_{\mathrm{M}}(\rho_1, \rho_2). \tag{D.4}$$

On the other hand consider the following transformation of the density H_{ρ_1} into H_{ρ_2}: we transport the 'mass' along each meridian separately (this is feasible due to assumption (1)) and then we join all the transformations together. Applying the Salvemini formula (3.4) to each meridian ($\varphi \in [0, 2\pi]$), averaging the results over $[0, 2\pi]$ and finally using assumption (2) we obtain

$$D_{\mathrm{M}}(\rho_1, \rho_2) \leqslant \frac{1}{2\pi} \int_0^{2\pi} \int_0^{\pi} |F_1(t, \varphi) - F_2(t, \varphi)|\, \mathrm{d}t\, \mathrm{d}\varphi = \tilde{D}_{\mathrm{M}}(\rho_1, \rho_2) \tag{D.5}$$

which completes the proof.

Appendix E. Derivation of the Monge distances for some interesting cases

E.1. Derivation of formula (4.14)

Let $j \in \mathbb{N}$ and $m = -j + 1, \ldots, j$. We put $N = 2j + 1$ and $n = j + m$. Applying proposition 5 and then the substitution $u = \cos^2(\vartheta/2)$ we obtain

$$\begin{aligned}D_{\mathrm{M}}(|j, m\rangle, |j, m-1\rangle) &= \int_0^{\pi} \left| \int_0^{y} G\big(n, N, \cos^2(\vartheta/2)\big) \right. \\ &\quad \left. - G\big(n-1, N, \cos^2(\vartheta/2)\big) (\sin\vartheta)/2\, \mathrm{d}\vartheta \right| \mathrm{d}y \\ &= \int_0^{\pi} \left| \int_{\cos^2 \frac{y}{2}}^{1} G(n, N, u) - G(n-1, N, u)\, \mathrm{d}u \right| \mathrm{d}y\end{aligned} \tag{E.1}$$

where $G(n, N, u) := N\binom{N-1}{n} u^n (1-u)^{(N-1-n)}$ for $u \in [0, 1]$. Using the identity

$$\int \big(G\big(n-1, N, u\big) - G(n, N, u)\big)\, \mathrm{d}u = \binom{N}{n} u^n (1-u)^{(N-n)} \tag{E.2}$$

we obtain

$$D_{\mathrm{M}}(|j,m\rangle, |j,m-1\rangle) = 2\binom{N}{n}\int_0^{\pi/2} \cos^{2n} v \sin^{2(N-n)} v \,\mathrm{d}v$$
$$= \binom{N}{n}\frac{\Gamma(n+1/2)\,\Gamma(N-n+1/2)}{\Gamma(N)}$$
$$= \pi\binom{2(N-n)}{N-n}\binom{2n}{n}2^{-2N} \sim \frac{1}{\sqrt{N-n}\sqrt{n}} \qquad \text{(E.3)}$$

as desired.

E.2. Derivation of formula (4.18)

For $j \in \mathbb{N}$ we put $D_j := D_{\mathrm{M}}(|j,0\rangle\langle j,0|, \rho_*)$. From proposition 5 and formula (4.7) we deduce that

$$D_j = \int_0^{\pi} \left| \int_0^{\vartheta} h_{|j,0\rangle\langle j,0|}(\psi)\,\mathrm{d}\psi - \int_0^{\vartheta} h_{\rho_*}(\psi)\,\mathrm{d}\psi \right| \mathrm{d}\vartheta$$
$$= \int_0^{\pi} \left| \int_0^{\vartheta} \left(G\left(\cos^2\left(\psi/2\right)\right) - 1\right)\tfrac{1}{2}\sin\psi\,\mathrm{d}\psi \right| \mathrm{d}\vartheta \qquad \text{(E.4)}$$

where $G(u) := (2j+1)\binom{2j}{j}u^j(1-u)^j$ for $u \in [0,1]$. Applying the substitutions $u = \cos^2(\psi/2)$ and $y = \vartheta/2$ and using the symmetry arguments yields

$$D_j = 2\int_0^{\pi/2} \left| \int_{\cos^2(\vartheta/2)}^{1} \left(G(u) - 1\right)\mathrm{d}u \right| \mathrm{d}\vartheta$$
$$= 2\int_0^{\pi/4} \int_{\sin^2 y}^{\cos^2 y} G(u)\,\mathrm{d}u\,\mathrm{d}y - 1$$
$$= 2(2j+1)\binom{2j}{j}\int_0^{\pi/4} \int_{\sin^2 y}^{\cos^2 y} u^j(1-u)^j\,\mathrm{d}u\,\mathrm{d}y - 1. \qquad \text{(E.5)}$$

Set $c_j(u) := 2(2j+1)\binom{2j}{j}\int u^j(1-u)^j\,\mathrm{d}u$ for $u \in [0,1]$, $j \in \mathbb{N}$. Then $D_j = \int_0^{\pi/4}\left(c_j\left(\cos^2 y\right) - c_j\left(\sin^2 y\right)\right)\mathrm{d}y - 1$. Integrating by parts we obtain $c_j(u) = 2\binom{2j}{j}(2u-1)\,u^j(1-u)^j + c_{j-1}(u)$, and so $D_j = \binom{2j}{j}2^{-2j}\frac{1}{2j+1} + D_{j-1}$. Moreover we can put $D_0 = 0$. Thus $D_j = \sum_{k=1}^{j}\frac{1}{2k+1}2^{-2k}\binom{2k}{k} = \sum_{k=1}^{j}\frac{1}{2k+1}\frac{(2k-1)!!}{(2k)!!}$, as claimed. Applying Taylor's formula $\arcsin x = \sum_{k=0}^{\infty}\frac{1}{2k+1}\frac{(2k-1)!!}{(2k)!!}x^{2k+1}$ we obtain $D_j \to \pi/2 - 1$ $(j \to \infty)$.

E.3. Derivation of formula (4.19)

Let $C(\Xi, j) = D_{\mathrm{M}}(\rho_+, \rho_\Xi)$ for $\Xi \in [0,\pi]$ and $j = 1/2, 1, \ldots$. It follows from the rotational invariance of the Monge metric (property B) that $C(\Xi, j) = D_{\mathrm{M}}(\rho_1, \rho_2)$, where $\rho_1 = \rho_{(\pi-\Xi)/2}$ and $\rho_2 = \rho_{(\pi+\Xi)/2}$. To apply proposition 6 observe first that according to formula (4.5) we have

$$H_{\rho_1}(\vartheta,\varphi) = (2j+1)\left(\frac{1+\sin\vartheta\cos(\Xi/2)\cos\varphi + \cos\vartheta\sin(\Xi/2)}{2}\right)^{2j} \qquad \text{(E.6)}$$

$$H_{\rho_2}(\vartheta,\varphi) = (2j+1)\left(\frac{1+\sin\vartheta\cos(\Xi/2)\cos\varphi - \cos\vartheta\sin(\Xi/2)}{2}\right)^{2j} \qquad \text{(E.7)}$$

and so $H_{\rho_1}(\vartheta,\varphi) = H_{\rho_2}(\pi-\vartheta,\varphi)$ for $(\vartheta,\varphi) \in S^2$. Thus, applying the substitution $\pi - \vartheta \to \vartheta$, we obtain $F_1(\pi,\varphi) = \frac{1}{2}\int_0^{\pi} H_{\rho_i}(\vartheta,\varphi)\sin\vartheta\,\mathrm{d}\vartheta = \frac{1}{2}\int_0^{\pi} H_{\rho_2}(\vartheta,\varphi)\sin\vartheta\,\mathrm{d}\vartheta =$

$F_2(\pi,\varphi)$, and $F_1(t,\varphi)-F_2(t,\varphi)=F_1(\pi-t,\varphi)-F_2(\pi-t,\varphi)$ for $t\in[0,\pi]$ and $\varphi\in[0,2\pi]$, which implies the assumption (1). Moreover, $H_{\rho_1}(\vartheta,\varphi)-H_{\rho_2}(\vartheta,\varphi)\geqslant 0$ for $\vartheta\in[0,\pi/2]$ and $\varphi\in[0,2\pi]$. From this fact and from the symmetry of the functions $F_1(\cdot,\varphi)-F_2(\cdot,\varphi)$ ($\varphi\in[0,2\pi]$) we deduce the assumption (2). Hence the assumptions of proposition 6 are fulfilled and we conclude that

$$C(\Xi,j)=\frac{2j+1}{\pi 4^{j+1}}\int_0^{2\pi}\int_0^{\pi}\left(\int_0^{t}\left((w+z)^{2j}-(w-z)^{2j}\right)\sin\vartheta\,\mathrm{d}\vartheta\right)\mathrm{d}t\,\mathrm{d}\varphi \tag{E.8}$$

where $w:=1+\sin\vartheta\cos(\Xi/2)\cos\varphi$ and $z:=\cos\vartheta\sin(\Xi/2)$. Applying the identity

$$(w+z)^{2j}-(w-z)^{2j}=\begin{cases}2z\displaystyle\sum_{k=0}^{j-1}\binom{2j}{2k+1}w^{2k+1}z^{2j-2k-2} & \text{for}\quad 2j\text{ —even}\\ 2z\displaystyle\sum_{k=0}^{j-1/2}\binom{2j}{2k}w^{2k}z^{2j-2k-1} & \text{for}\quad 2j\text{—odd}\end{cases} \tag{E.9}$$

and performing the integration we obtain after tedious (but elementary) calculation the desired result.

References

[1] Hillery M 1987 *Phys. Rev.* A **35** 725
[2] Hillery M 1989 *Phys. Rev.* A **39** 2994
[3] Englert B G 1996 *Phys. Rev. Lett.* **77** 2154
[4] Knöll L and Orłowski A 1995 *Phys. Rev. Lett.* A **51** 1622
[5] Wünsche A 1995 *Appl. Phys.* B **60** S119
[6] Dodonov V V, Man'ko O V, Man'ko V I and Wünsche A 1999 *Phys. Scr.* **59** 81
[7] Bures D J C 1969 *Trans. Am. Math. Soc.* **135** 199
[8] Uhlmann A 1976 *Rep. Math. Phys.* **9** 273
[9] Hübner M 1992 *Phys. Lett.* A **163** 239
[10] Uhlmann A 1996 *J. Geom. Phys.* **18** 76
[11] Dittmann J 1995 *Rep. Math. Phys.* **36** 309
[12] Petz D and Sudár C 1996 *J. Math. Phys.* **37** 2662
[13] Uhlmann A 1995 *Rep. Math. Phys.* **36** 461
[14] Slater P B 1996 *J. Phys. A: Math. Gen.* **29** L271
[15] Dittmann J 1999 *J. Phys. A: Math. Gen.* **32** 2663
[16] Lesniewski A and Ruskai M B 1999 *J. Math. Phys.* **40** 5702
[17] Braunstein S L and Caves C M 1994 *Phys. Rev. Lett.* **72** 3439
[18] Wootters W K 1981 *Phys. Rev.* D **23** 357
[19] Brody D C and Hughston L P 2001 *J. Geom. Phys.* **38** 19
[20] Życzkowski K and Słomczyński W 1998 *J. Phys. A: Math. Gen.* **31** 9095
[21] Życzkowski K, Słomczyński W and Wiedemann H 1993 *Vistas Astron.* **37** 153
[22] Husimi K 1940 *Proc. Phys. Math. Soc. Japan* **22** 264
[23] Dodonov V V, Man'ko O V, Man'ko V I and Wünsche A 2000 *J. Mod. Opt.* **47** 633
[24] Adelman M, Corbett J V and Hurst C A 1993 *Found. Phys.* **23** 211
[25] Boya L J, Byrd M, Mims M and Sudarshan E C G 1998 *Preprint* arXiv quant-ph/9810084
[26] Życzkowski K, Horodecki P, Sanpera A and Lewenstein M 1998 *Phys. Rev.* A **58** 883
[27] Slater P 1998 *J. Phys. A: Math. Gen.* **32** 5261
[28] Życzkowski K 1999 *Phys. Rev.* A **60** 3496
[29] Poźniak M, Życzkowski K, and Kuś M 1998 *J. Phys. A: Math. Gen.* **31** 1059
[30] Hardy G H and Ramanujan S S 1918 *Proc. Lond. Math. Soc.* **17** 75
[31] Cassinelli G and Lahti P J 1993 *Bridging the Gap: Philosophy, Mathematics, and Physics* ed G Corsi *et al* (Berlin: Springer) pp 211–24
[32] Bush P, Cassinelli G and Lahti P J 1995 *Rev. Math. Phys.* **7** 1105
[33] Bengtsson I 1998 Geometry of quantum mechanics *Preprint*
[34] Monge G 1781 Mémoire sur la théorie des déblais et des remblais *Histoire de l'Academie des Sciences de Paris* p 666

[35] Rachev S T 1984 *Theor. Prob. Appl.* **29** 647
[36] Rachev S T 1991 *Probability Metrics and the Stability of Stochastic Models* (New York: Wiley)
[37] Sudakov V N 1976 *Tr. Mat. Inst. V. A. Steklov, Akad. Nauk SSSR* **141** (in Russian)
[38] Evans L C and Gangbo W 1999 *Mem. Am. Math. Soc.* **137**
[39] Kantorovich L V 1942 *Dokl. Akad. Nauk SSSR* **37** 227
[40] Kantorovich L V 1948 *Usp. Mat. Nauk* **3** 225
[41] Rachev S T and Rüschendorf L 1998 *Mass Transportation Problems Vol. I. Theory* (New York: Springer)
[42] Kantorovich L V 1939 Mathematical methods in the organization and planning of production (Leningrad State University: Leningrad) translated in 1990 *Manage. Sci.* **6** 366
[43] Salvemini T 1943 *Atti della VI Riunione della Soc. Ital. di Statistica* (Roma)
[44] Wiedemann H, Życzkowski K and Słomczyński W 1998 *Frontiers in Quantum Physics* ed S C Lim *et al* (Berlin: Springer) pp 240–4
[45] Wu N and Coppins R 1981 *Linear Programming and Extensions* (New York: McGraw-Hill)
[46] Perelomov A 1986 *Generalized Coherent States and Their Applications* (Berlin: Springer)
[47] Thirring W 1980 *Lehrbuch der Mathematischen Physik. Band 4: Quantenmechanik grosser Systeme* (Springer: Wien)
[48] Rieffel M A 1999 *Doc. Math.* **4** 559
(Rieffel M A 1999 *Preprint* arXiv math.OA/9906151)
(Rieffel M A 2000 *Preprint* arXiv math.OA/0011063)
[49] Radcliffe J M 1971 *J. Phys. A: Math. Gen.* **4** 313
[50] Arecchi F T, Courtens E, Gilmore R and Thomas H 1972 *Phys. Rev.* A **6** 2211
[51] Zhang W-M, Feng D H and Gilmore R 1990 *Rev. Mod. Phys.* **62** 867
[52] Vieira V R and Sacramento P D 1995 *Ann. Phys., NY* **242** 188
[53] Majorana E 1932 *Nuovo Cimento* **9** 43
[54] Bacry H 1974 *J. Math. Phys.* **15** 1686
[55] Penrose R 1994 *Shadows of the Mind* (Oxford: Oxford University Press)
[56] Lebœuf P and Voros A 1990 *J. Phys. A: Math. Gen.* **23** 1765
[57] Słomczyński W and Życzkowski K 2001 in preparation
[58] Barros e Sá N 2001 *J. Phys. A: Math. Gen.* **34** 4831
(Barros e Sá N 2000 *Preprint* arXiv quant-ph/0009022)
[59] Bogomolny E, Bohigas O and Lebœuf P 1992 *Phys. Rev. Lett.* **68** 2726
[60] Wehrl A 1979 *Rep. Math. Phys.* **16** 353
[61] Lieb E H 1978 *Commun. Math. Phys.* **62** 35
[62] Scutaru H 1979 *preprint* FT-180/1979
Scutaru H 1999 *Preprint* arXiv math-ph/9909024
[63] Lee C-T 1988 *J. Phys. A: Math. Gen.* **21** 3749
[64] Schupp P 1999 *Commun. Math. Phys.* **207** 481
[65] Gnutzmann S and Życzkowski K 2001 *Preprint* arXiv quant-ph/0106016
[66] Kuś M, Mostowski J and Haake F 1988 *J. Phys. A: Math. Gen.* **21** L1073
[67] Jones K R W 1990 *J. Phys. A: Math. Gen.* **23** L1247
[68] Słomczyński W and Życzkowski K 1998 *Phys. Rev. Lett.* **80** 1880
[69] Życzkowski K 2001 *Physica* E **9** 583
[70] Haake F, Wiedemann H and Życzkowski K 1992 *Ann. Phys., Lpz.* **1** 531
[71] Haake F 2000 *Quantum Signatures of Chaos* 2nd edn (Berlin: Springer)
[72] Żurek W H 1981 *Phys. Rev.* D **24** 1516
[73] Żurek W H 1998 *Phys. Scr.* T **76** 186
[74] Hannay J H 1996 *J. Phys. A: Math. Gen.* **29** L101